Utah State University
DigitalCommons@USU

All Graduate Theses and Dissertations | Graduate Studies

5-2015

Effect of Manufacturing Processes on the Loss Factor and Other Mechanical Properties of Kenaf Fiber-Reinforced Composites

Brian P. Spackman
Utah State University

Follow this and additional works at: https://digitalcommons.usu.edu/etd

 Part of the Mechanical Engineering Commons

Recommended Citation

Spackman, Brian P., "Effect of Manufacturing Processes on the Loss Factor and Other Mechanical Properties of Kenaf Fiber-Reinforced Composites" (2015). *All Graduate Theses and Dissertations*. 4256.
https://digitalcommons.usu.edu/etd/4256

This Thesis is brought to you for free and open access by the Graduate Studies at DigitalCommons@USU. It has been accepted for inclusion in All Graduate Theses and Dissertations by an authorized administrator of DigitalCommons@USU. For more information, please contact digitalcommons@usu.edu.

EFFECT OF MANUFACTURING PROCESSES ON THE LOSS FACTOR AND OTHER MECHANICAL PROPERTIES OF KENAF FIBER-REINFORCED COMPOSITES

by

Brian P. Spackman

A thesis submitted in partial fulfillment
of the requirements for the degree

of

MASTER OF SCIENCE

in

Mechanical Engineering

Approved:

Dr. Thomas Fronk Major Professor	Dr. Ling Liu Committee Member
Dr. Jason Quinn Committee Member	Dr. Mark R. McLellan Vice President for Research and Dean of the School of Graduate Studies

UTAH STATE UNIVERSITY
Logan, Utah

2015

Copyright © Brian P. Spackman 2015

All Rights Reserved

ABSTRACT

Effect of Manufacturing Processes on the Loss Factor and Other Mechanical Properties of Kenaf Fiber-Reinforced Composites

by

Brian P. Spackman, Master of Science

Utah State University, 2015

Major Professor: Dr. Thomas Fronk
Department: Mechanical and Aerospace Engineering

Kenaf fibers have mechanical properties making them a good candidate to replace glass fibers in composites. This research investigates kenaf fiber-reinforced composites, examining the effect of cure time, density, matrix hardener ratio, surface treatment, and fiber length on the mechanical properties of the composite material such as natural frequency, damping loss factor, and tensile modulus. These are essential characteristics for many manufacturing parts and products, but are not well known for natural fiber-reinforced composite materials since interest in utilizing natural fibers for composites is in the infancy phase and determining properties is difficult. Natural fibers display properties similar to glass fibers, and present a more environmentally friendly option for manufacturing composite materials. By studying published research on the topic and experimenting with different methods, a consistent procedure for manufacturing composites was

developed and several samples were created for testing these parameters. These samples were subjected to a vibrational test using an impact hammer and accelerometer. Through the half-power bandwidth method and other relationships, mechanical properties were extracted from the test to study the effect of each manufacturing process. Samples were found to exhibit repeatable mechanical properties after approximately 150 hours following removal from the oven. Increasing the pressure applied during the cure cycle results in higher densities, which increases loss factors and tensile moduli, and lowers natural frequencies. The matrix hardener ratio also affects these properties in a similar way. High hardener ratios result in a more brittle material that dampens less but generally has a higher stiffness. Models predict that a chemical surface treatment should decrease the loss factor due to a better fiber-matrix bond, resulting in less sliding and friction. However, testing showed the opposite result with treated fibers exhibiting higher amounts of damping. Fiber length was also tested, though the results showed a less prominent effect.

(95 pages)

PUBLIC ABSTRACT

Effect of Manufacturing Processes on the Loss Factor and Other Mechanical Properties of Kenaf Fiber-Reinforced Composites

Brian P. Spackman, Master of Science

The characteristics essential for manufacturing parts and products are not well known for natural fiber-reinforced composite materials. Natural fibers display properties similar to glass fibers, and present a more environmentally friendly option for manufacturing composite materials. This research investigates various parameters in the manufacture of kenaf fiber-reinforced composites including cure time, density, matrix hardener ratio, surface treatment, and fiber length and examines the effect they have on mechanical properties of the composite material. Several samples were created and subjected to a vibrational test. Using known relationships, mechanical properties were extracted from the test results. Samples were found to exhibit repeatable mechanical properties after approximately 150 hours following removal from the oven. Increasing the pressure applied during the cure cycle results in higher densities, which increases damping and stiffness. The matrix hardener ratio also affects these properties in a similar way. High hardener ratios result in a more brittle material that dampens less but generally has a higher stiffness. Testing showed that chemically treated fibers exhibit higher amounts of damping. Fiber length was also tested, though the effect was less prominent.

ACKNOWLEDGMENTS

My appreciation goes to Utah State University for building a great mechanical engineering program and beautiful institution. The memories made and lessons learned on this campus are ones I cherish. I offer immense gratitude to my major professor, Dr. Thomas Fronk, for his continued guidance and support during the developing, testing, and reporting processes.

I am grateful to the United States Air Force, my current employer, who has provided financial support and time off to work on my studies and research. What a blessing it has been to focus my full attention on academics.

Finally, the words *thank you* hardly touch the gratitude I feel for my family. They have been the greatest teachers throughout my life. They have made me better academically, but more importantly, they have taught me to be morally upright, considerate, and hardworking. Their examples and teachings have given me confidence to reach for the most important goals in my life.

Brian P. Spackman

CONTENTS

Page

LIST OF TABLES

LIST OF FIGURES

NOMENCLATURE

A	Cross-Sectional Area
E	Tensile Modulus
E_x'	Storage Tensile Modulus
E_x''	Loss Tensile Modulus
F	Forcing Function
G_x'	Storage Shear Modulus
G_x''	Loss Shear Modulus
i	Imaginary Number
I	Moment of Inertia
k	Spring Constant
l	Length
m	Mass
r_x	Radius
t	Time
V_x	Volume Fraction
x	Position
X	Amplitude of Position
$\ddot{x}$	Acceleration
α	Phase Angle
$\beta_n l$	Boundary Condition Constant
ϵ	Strain
η_x	Loss Factor

ρ	Density
σ	Stress
ω	Frequency
ω_n	Natural Frequency

CHAPTER 1

INTRODUCTION

Natural fibers have been identified as a great opportunity to make composite materials more sustainable as well as green since they come from natural products and are biodegradable for a clean end of life disposal. The properties of several natural fibers are comparable to glass fibers, making them a suitable replacement for certain applications [1]. One natural fiber showing great potential is kenaf. However, some kenaf fiber properties and particularly the mechanical properties of the composites manufactured from them are not well known. Information regarding damping characteristics is especially lacking. To begin large scale use of natural fibers, the fiber and composite properties need to be established with repeatable test results. Test results vary widely because of the inconsistent properties of the fibers themselves. Natural fibers, unlike manufactured fibers such as carbon or glass fibers, do not have a constant cross-section but instead contain variability in the radial and axial directions. The fibers are anisotropic and come in short lengths which vary from one fiber to the next. For these reasons, determining consistent properties and results is difficult. This paper outlines parameters that are known, compares kenaf fibers to currently produced glass and carbon fibers, and determines damping characteristics of kenaf fiber-reinforced composites, discussing the manufacturing processes that influence damping based on both calculations and material testing.

CHAPTER 2

BACKGROUND INFORMATION

2.1 Natural Fiber Composites

Composite materials are becoming more and more essential in progressive designing because of their low density, low cost, and good mechanical properties [2],[3]. They combine the properties of the fiber and matrix materials to produce a new range of properties not available by either component alone. The fiber adds strength and stiffness while the matrix holds the fibers together making them better for load bearing and offers the structure compliance. This allows for tailoring of the product to meet specific requirements. Natural fibers are especially desirable because they are renewable (implying a theoretical limitless supply) and biodegradable materials [4],[5]. In addition, the live plants absorb airborne carbon dioxide, capturing it. There are vast amounts of agroproduct generated and unused every year, leaving an abundant supply of material to be tapped into and a chance to eliminate waste [6]. Kenaf has been designated as a great candidate for use as a biofiber in composite materials. It has the advantages listed above for traditional composite fibers with similar properties to E-glass fibers at a potentially competitive cost [7]. Current production cannot compete economically with current glass fiber composites, but the costs will reduce dramatically with increased production rates and more efficient processes. The environmentally friendly nature

of these fibers leads to their designation as green composites and sets them apart from traditional fiber materials.

Fibers from several plants, including kenaf, flax, hemp, and jute to name a few, have been identified and tested for advantageous mechanical properties. Kenaf fibers come from the Hibiscus cannabinus plant and have received much attention as reinforcement for thermoplastic and thermosetting polymers in developing new composite materials [8],[9]. This interest is merited by its favorable material properties. Figure 1 compares kenaf to other common natural fibers. All fibers have similar density while kenaf has the highest tensile strength and second highest tensile modulus.

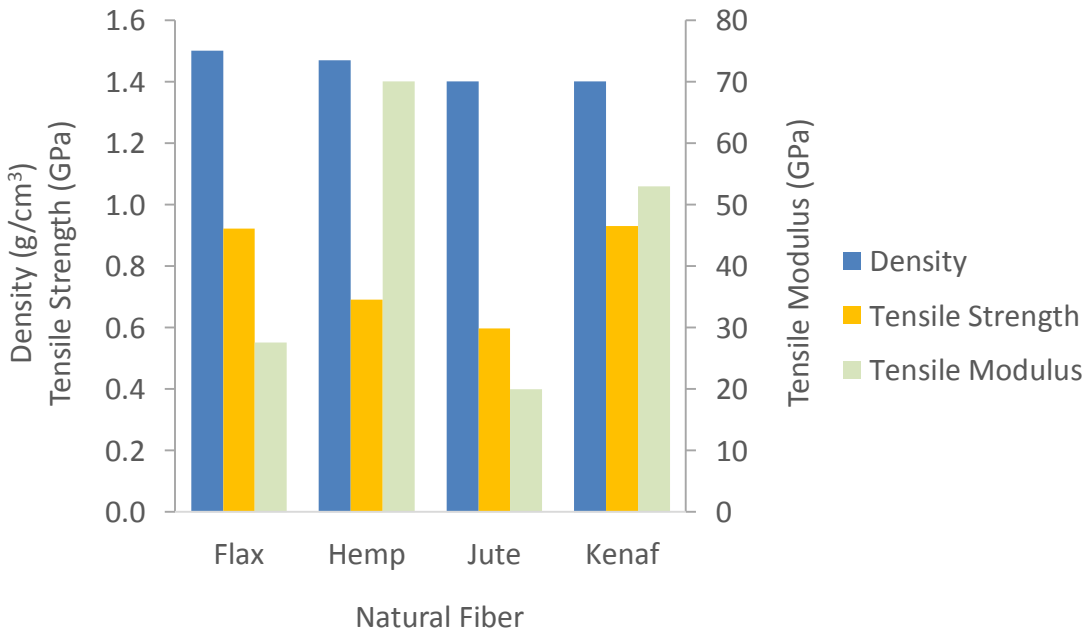

Figure 1: Comparison of Natural Fiber Properties

Many fiber properties vary depending on cultivation location as well as the portion of the plant harvested, but general properties have been established such as fiber diameter, length, density, etc. [2],[10]. Properties are more difficult to define for natural fibers due to their irregular, nonhomogeneous, and anisotropic nature. Nevertheless, attempts are made to represent the fibers as consistent, homogeneous, isotropic materials. Typical reported properties for kenaf fibers are listed in Table 1 [1],[10]. However, the composite properties are much more variable and lack concrete, research-backed property data.

Table 1: Reported Properties of Kenaf Fibers

Property	Value
Fiber Diameter	5 - 15 μm
Bundle Diameter	50 – 200 μm
Possible Length	500 mm
Density	1.4 kg/m^3
Tensile Modulus	53 GPa
Ultimate Tensile Strength	930 MPa

Akil et al. have summarized the considerable research devoted to determining the mechanical properties of nonrenewable fiber reinforced composites, but there is a current lack of information regarding natural fiber reinforced composite materials [1]. This deficiency is especially evident in damping characteristics due to insufficient testing in this area. Repeatable, reliable, and well-defined mechanical properties will encourage the advancement of biofiber design and ensure the integrity of such designs [3]. Published research shows considerable inconsistency,

a general deficit in properties, and a vast range of reported values. The widely varying results are in part due to the anisotropic nature of the fibers. The fibers themselves are not isotropic, varying in size and properties in both the radial and axial directions. The results also vary based on plant properties arising from differences in location of growth, climate of the area, and time length of growth, as well as insufficient testing and concrete measurements to firmly establish the properties [11].

2.2 Description of Components

Composite materials are composed of fibers embedded in a matrix. However, they contain three regions worth examining, the fibers, the matrix, and the interface as depicted in Figure 2. All three interact, determining the mechanical properties of the composite.

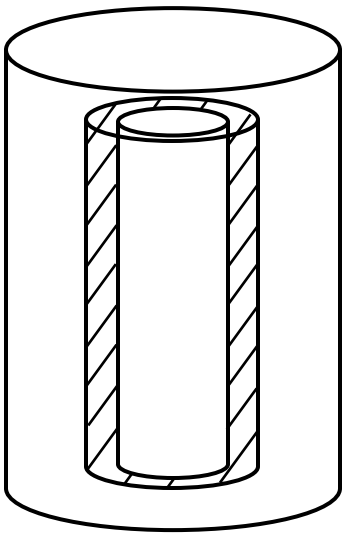

Figure 2: Model of Fiber (Inner), Interphase (Striped), and Matrix (Outer)

The fibers in a composite provide the strength and carry most of the load. Fibers are made from numerous materials including polymers, glass, carbon, graphite, Kevlar, and biomaterial [12]. Glass and carbon fibers are most commonly used in industry. Composites can be either axially aligned, meaning all fibers in a layer run the same direction, or they can be randomly oriented. Manufactured fibers such as carbon can be formed into very long strands and work well for axially aligned composites. However, biofibers are difficult to produce in strands that are long enough to orient. Therefore, natural fiber-reinforced composites are generally created with randomly oriented fibers. The inconsistent, non-homogeneous nature of kenaf fibers make them difficult to manufacture and problematic to test and analyze.

The matrix bonds the fibers together and helps transfer a load between fibers allowing the composite to handle significant loads. Several materials can be used as a matrix including polymers, metals, or ceramics. Polymers are the most commonly used and are further distinguished as thermoplastics, thermosets, and rubbers. A major difference between thermoplastics and thermosets is that the prior can be softened by applying heat and hardened again through cooling, while the latter cannot be softened by heating, instead forming chemical reactions and setting into a form that is not reversible [13]. The matrix holds the fibers in place and in proper alignment, maintaining the overall shape of the composite material. It also transfers the load to the fibers and protects the fibers from corrosion and abrasion [12]. The

matrix is critical in assessments, but the fibers, matrix, and interface are all examined in determining the performance of a composite material [14].

The interface is the region where the bonding occurs between the matrix and fibers. This region transfers the load between matrix and fiber making the properties of each very important. However, a poor bond at the interface will lead to debonding and an ineffective composite material. This region is referred to as the interface if it is assumed to be a sizeless, volumeless boundary, but called interphase if there is a transition region between the fiber and matrix that contains its own distinct mechanical properties. This region may be small for certain applications but has been found to be large and influential for many composites [15],[16]. Treating the fibers with chemicals prior to bonding improves bond strength between the fibers and matrix. The surface treatments vary depending on the fiber type, but correct physical or chemical treatments increase overall composite properties [17],[18].

2.3 Hydrophilic Nature of Fibers

Most reinforcing fibers, including the two most common (glass and carbon), tend to be hydrophobic in nature. A major problem arises in natural, cellulose based, fibers because of their hydrophilic nature compared to the hydrophobic nature of most matrix materials [19]. The fibers absorb moisture, altering the overall mechanical properties of the fibers and therefore the entire composite material [4]. This leads to a poor interface bond and decreased strength in the

composite. Several physical and chemical treatments have been found to aid in reducing this water absorbing tendency by altering the fiber surface properties [20].

A common method for treating fibers involves subjecting them to chemical treatments. Sodium Hydroxide (NaOH) is one of the most common and effective chemicals for treating natural fibers, especially kenaf, so it was selected for this research [20]. It falls under the category of alkaline treatments, and provides several advantages by reacting with the fiber's hydrophilic hydroxyl group [19]. The chemicals serve two purposes, namely cleaning and etching the fibers. When applied in an aqueous solution, NaOH eliminates stray particles and cleans the surface of the fibers. In addition, it etches the fiber surface, thereby increasing the surface roughness to promote physical and reaction-based bonding. This enhances fiber-fiber and fiber-matrix bonding, and improves tensile properties and fatigue characteristics. Current research recommends NaOH aqueous solutions ranging from one to ten percent for time periods ranging from minutes to hours [6],[19],[20].

2.4 Possible Applications

The most common materials for reinforcing composite materials include carbon and glass fibers. Natural fibers cannot compete with carbon fibers, which have a very high tensile modulus and tensile strength. However, Table 2 shows that glass fibers and natural fibers are more comparable in these properties, especially in

specific stiffness and specific strength, making it feasible to replace glass fibers with natural fibers in certain applications [1],[21].

Table 2: Comparison of Kenaf, Glass, and Carbon Fiber Properties

Fibers	Density (kg/m^3)	Tensile Modulus (GPa)	Tensile Strength (MPa)
Kenaf	1.4	53	930
E-Glass	2.55	73	2400-3400
Carbon	1.78	240-425	3400-4800

There are several applications available for biofiber-reinforced composites. For example, it offers the automotive industry a viable low-cost alternative to fiberglass in areas where low-weight, impact damping materials are needed. Damping is a very important characteristic in design. Energy is absorbed by all materials in varying amounts due to material damping during cyclic deformation [22]. Determining what material to use in a given situation requires firm knowledge about the damping capability. Several automobile components have been listed as potential parts for natural fiber reinforced composites including vehicle doors, instrument panels, and engine covers [3]. Davoodi et al. researched the advantage and feasibility of designing a completely eco-friendly car bumper beam. This part requires an energy absorption process to dampen the dangerous impact of a collision, and biofibers have the potential to replace glass fibers in this part if the mechanical characteristics become more repeatable and well-defined [5].

Several other applications have been identified [6],[20], and finding additional applications to consume high quantities of natural fiber-reinforced composites is a major pursuit that would be accelerated with greater understanding of the fiber and composite properties. Such applications would create a demand, allowing natural fibers to compete economically with glass and carbon based fibers [23]. Use of bioproducts in design of goods and consumables is not a novel idea nor is it a new area of study. For years products were made with renewable resources and studies focused on this production, but success in the petroleum industry deterred continued growth in this field [7],[23]. However, increased interest in the environment, a better understanding of the interconnectivity of environmental factors, and recent breakthroughs in biologically friendly material studies have led to a renewed effort to develop this field of study. Continuing to develop understanding of natural materials and finding large scale applications will make environmentally friendly composites a cost-effective, renewable, and reliable resource for design.

CHAPTER 3

SYSTEM MODEL AND CALCULATIONS

3.1 Three-Phase System Model

Damping is the mode whereby vibrational energy is converted into heat or sound. Many forms of damping exist. The material or hysteretic damping consists of energy being absorbed and dissipated by internal friction in the material when it is deformed [24]. Hysteretic damping in these materials is often idealized and approximated with good accuracy by representing it with an equivalent viscoelastic damping method [16],[25]. Natural fiber-reinforced composites can be modeled as viscoelastic materials. Amount of damping is frequently quantified and compared by defining a loss factor of the material as the energy dissipated per cycle of deformation. The method for obtaining this loss factor is described in the following section.

Single fiber-matrix composites have been modeled using several methods to include the theory of elasticity, finite element models, the cylinder theory, and the energy method, each with its individual set of benefits and limitations [15]. Early studies have modeled the composite as a two-phase material, representing the fiber and matrix materials, but recent studies have noted the importance of the interphase region which exists at the fiber-matrix interface region. There still remains much ambiguity in the properties of this interphase region, making precise modeling complex, but the importance of the interphase region in stress transfer as

well as damping and stiffness characteristics has been established [26]-[28]. A perfect interface without an interphase region can hardly be realized in actual composites. The interphase region is created by interactions between matrix and fiber constituents and has properties different from the matrix or fiber [15],[16].

Literature shows that stiff interphase properties are often assumed, meaning the interphase properties equal the average between the fiber and the matrix elastic properties [28]. Other literature assumes a soft interphase, with interphase properties assumed lower than those of the matrix. Gohil and Shaikh define this as one-tenth the average between the fiber and matrix properties [27],[28]. This variance in assumptions is due to the lack of literature to provide a precise estimation of the interphase properties. The interphase region is very small and not possible to separate and test individually, making it very difficult to know its properties with any certainty.

3.2 Storage and Loss Moduli

The loss factor can also be determined by assuming a complex modulus for the material. Thus the stress strain equation becomes

$$\sigma = (E' + E''i)\epsilon. \tag{3.1}$$

In this equation, E' is the storage modulus and E" is the loss modulus. The loss factor is the ratio of the loss modulus to the storage modulus, or

$$\eta = \frac{E''}{E'}. \tag{3.2}$$

The DMA can find values for the storage and loss moduli.

3.3 Model of Composite Loss Factor

From the energy method, a micromechanical model can be created to predict the damping characteristics of natural fiber-reinforced composites, accounting for the fiber, matrix, and interphase regions. The following method is offered for determining the damping loss factor based on a three-phase model of a composite material [22]. A control volume for this method is represented in Figure 3. The model suggests that the loss factor is a function of the fiber, matrix, and interphase properties.

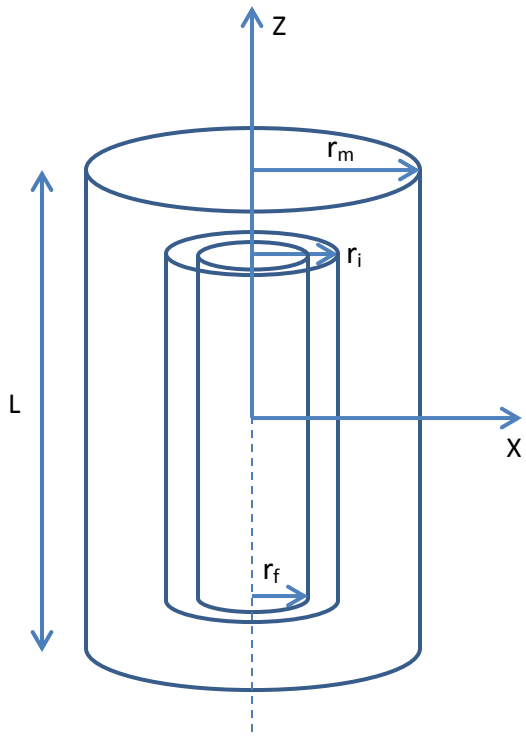

Figure 3: Energy Method Model Depiction and Parameters

Four assumptions are made for this model, namely that a perfect bond exists at all interfaces, that the fiber and matrix can only carry stresses normal to the fiber, that the interphase can only carry shear stresses, and that the fiber, matrix, and interphase materials are homogeneous and isotropic. Though these simplifications are not completely accurate, they are reasonable and will be accepted for the analytical examination of the system.

This method builds from the previously established formula for loss factor in equation 3.2. In addition, it offers a technique for obtaining E_c' and E_c'', the composite specimen's storage and loss moduli respectively.

$$E_c' = E_f' V_f \left[1 - \frac{\tanh\left(\frac{\beta l}{2}\right)}{\frac{\beta l}{2}}\right] - \frac{E_f'' V_f}{2}\left(\eta_i - \eta_f\right)\left[\frac{\tanh\left(\frac{\beta l}{2}\right)}{\frac{\beta l}{2}} - \frac{1}{\cosh^2\left(\frac{\beta l}{2}\right)}\right] + E_m' V_m \qquad (3.3)$$

$$E_c'' = E_f'' V_f \left[1 - \frac{\tanh\left(\frac{\beta l}{2}\right)}{\frac{\beta l}{2}}\right] + \frac{E_f' V_f}{2}\left(\eta_i - \eta_f\right)\left[\frac{\tanh\left(\frac{\beta l}{2}\right)}{\frac{\beta l}{2}} - \frac{1}{\cosh^2\left(\frac{\beta l}{2}\right)}\right] + E_m'' V_m \qquad (3.4)$$

Here, E_f' and E_f'' are the storage and loss moduli for the fiber and E_m' and E_m'' are the storage and loss moduli for the matrix. V_f and V_m are the fiber and matrix volume fractions, l is the length of the fibers, while η_i and η_f are the interphase and fiber loss factors being defined as

$$\eta_i = \frac{G_i''}{G_i'} \qquad (3.5)$$

and

$$\eta_f = \frac{E_f''}{E_f'}. \qquad (3.6)$$

The term β comes from the equation

$$\beta^2 = \frac{G'_m}{E'_f} * \frac{2}{r_f^2 \ln\left(\frac{r_m}{r_f}\right)} \tag{3.7}$$

where r_f is the radius of the fiber and r_m is the radius of the matrix control volume.

Current studies suggest that the majority of energy loss takes place in the matrix or the interphase regions. Therefore, the amount of energy lost in the fiber is very small compared to the amount lost in the other two regions. If the fiber loss factor is neglected, meaning the loss modulus is set to zero and the storage modulus is assumed to equal the tensile modulus, then equations 3.3 and 3.4 become

$$E'_c = E_f V_f \left[1 - \frac{\tanh\left(\frac{\beta l}{2}\right)}{\frac{\beta l}{2}}\right] - 0 + E'_m V_m \tag{3.8}$$

$$E''_c = 0 + \frac{E_f V_f}{2}(\eta_i)\left[\frac{\tanh\left(\frac{\beta l}{2}\right)}{\frac{\beta l}{2}} - \frac{1}{\cosh^2\left(\frac{\beta l}{2}\right)}\right] + E''_m V_m. \tag{3.9}$$

The loss factor can then be written as

$$\eta_c = \frac{\left(\frac{E_f V_f \eta_i}{2}\right)\left[\frac{\tanh\left(\frac{\beta l}{2}\right)}{\frac{\beta l}{2}} - \frac{1}{\cosh^2\left(\frac{\beta l}{2}\right)}\right] + E''_m V_m}{V_f\left[1 - \frac{\tanh\left(\frac{\beta l}{2}\right)}{\frac{\beta l}{2}}\right] + E'_m V_m} \tag{3.10}$$

from which the interphase loss factor, η_i, can be solved. This method offers more insight into the interphase region's properties, which are extremely difficult to isolate and measure due to the size of the interphase as well as large variances in this region. These complications make it challenging to filter out the effect of the interphase on overall damping.

3.4 Sensitivity Analysis on Loss Factor

These equations were implemented into a FORTRAN code to calculate the loss factor. The fiber and matrix properties are at least somewhat defined with some research, but the interphase properties are not known and present the most uncertainty as an input. The input properties were determined from published data as well as local University research testing. The following parameters listed in Table 3 were evaluated to determine the loss factor.

Table 3: Properties Used for Sensitivity Baseline Calculations

Parameter	Value	Units
Fiber Length ($\boldsymbol{l}$)	25	mm
Fiber Radius ($\boldsymbol{r_f}$)	25	μm
Matrix Radius ($\boldsymbol{r_m}$)	45	μm
Fiber Volume Fraction ($\boldsymbol{V_f}$)	0.3	--
Matrix Volume Fraction ($\boldsymbol{V_m}$)	0.6	--
Interphase Volume Fraction ($\boldsymbol{V_i}$)	0.1	--
Fiber Storage Modulus ($\boldsymbol{E'_f}$) [29]	3.0	GPa
Fiber Loss Modulus ($\boldsymbol{E''_f}$) [29]	0.18	GPa
Matrix Storage Modulus ($\boldsymbol{E'_m}$)	3.0	GPa
Matrix Loss Modulus ($\boldsymbol{E''_m}$)	0.15	GPa
Matrix Storage Shear Modulus ($\boldsymbol{G'_m}$) [30]	1.3	MPa
Interphase Storage Shear Modulus ($\boldsymbol{G'_i}$)	1.0	MPa
Interphase Loss Shear Modulus ($\boldsymbol{G''_i}$)	0.1	MPa

A sensitivity analysis was performed by altering each input parameter by ten percent and comparing the new loss factor to that obtained by the original parameters. JMP software was used to analyze the statistical influence each

parameter has on the loss factor. Figure 4 shows which properties have a statistically significant effect on the loss factor based on 80% and 90% confidence intervals for a two-tail t-distribution. For this 12 degree of freedom system, these confidence intervals correspond to critical t ratios of 1.78 and 1.36, respectively.

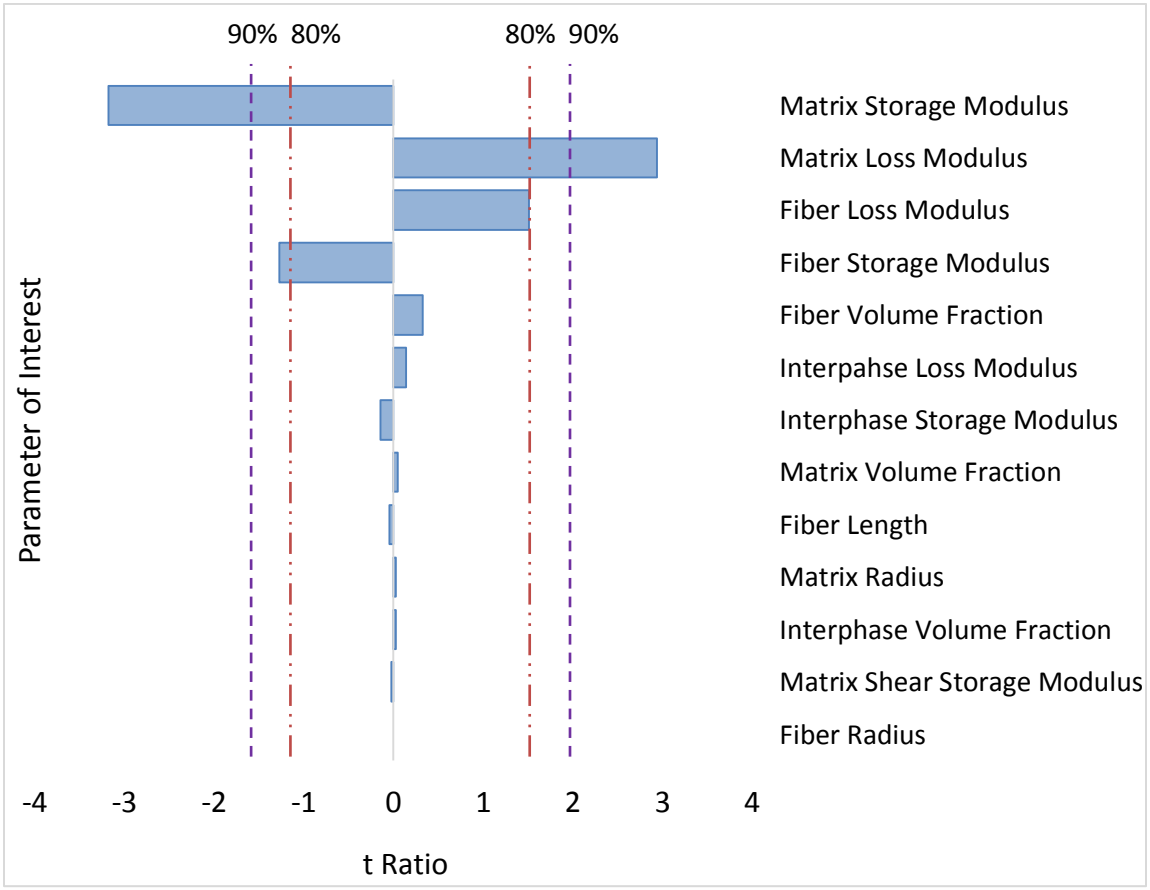

Figure 4: Sensitivity Analysis—Probability Significance of a Ten Percent Change in Listed Parameters on the Loss Factor for a Two-Tail t-Distribution

The 90% confidence interval indicates that the matrix material properties (storage and loss moduli) have the largest influence on the overall damping of the system. The fiber loss and storage moduli have the next largest effect, and the

interphase stiffness properties impact the loss factor the least. This suggests that even though the interphase property values contain the most uncertainty, according to these equations they should not influence the final results as much. However, coming up with an approximate value for the interphase properties, especially loss factor would help determine whether or not this is accurate. Recall that this model assumes a perfect bond between fibers and matrix, which is inaccurate for real specimens. The interphase region and the fiber to matrix bonding is not perfect and is influenced by the manufacturing process, especially chemical treatments on the fibers. Since the bond transfers stress between the matrix and fibers, alteration to the fiber-matrix boundary and bonding will change the interphase properties and thus influence the overall properties of the composite.

CHAPTER 4

TESTING METHOD AND TEST SETUP

4.1 Procedure for Laying Composites

The best way to prepare, lay out, and cure natural fiber-reinforced composites has not been definitively determined. Many issues arise with natural fibers that are absent from carbon or glass fibers. One issue, the hydrophilic nature of the fibers, has already been discussed. Other difficulties arise from the non-uniform cross-section of kenaf fibers. The fibers are not long and continuous like carbon fibers, nor do they stack neatly and evenly the way glass or carbon fibers do.

These factors, along with the anisotropic nature of the fibers and the variability from one fiber to the next, create considerable difficulty in producing a uniform specimen. Therefore, some testing was required to find an effective and repeatable way to create the composite materials. The best results (best tensile strength, highest density, most aesthetically pleasing) have been obtained using the following technique.

The fibers are chopped to a length of approximately ten millimeters. Once chopped, the fibers are soaked in a 5% solution of Sodium Hydroxide (NaOH) for approximately one hour, a concentration and timing chosen based on published research and local testing at Utah State University [31]-[33]. The NaOH solution alters the surface of the fibers, allowing for better bonding to the matrix. Following the chemical bath, the fibers are rinsed in distilled water to eliminate extraneous

material and remove the NaOH, halting further etching of the fiber surface. The fibers are then allowed to dry completely and separated from clumped bundles.

Once the fibers have been prepared, they are laid on a non-stick surface and a 100:27 weight volume mixture of epoxy to hardener is applied by hand. Figure 5 shows the chopped fibers and resin used. The epoxy chosen for this project is PT2050A and PT2050B1 hardener from PTM&W, Inc. Of the several matrix materials available, this was chosen because of its favorable tensile and flexural strength compared to other resins.

Figure 5: Chopped Fibers (left) and PT2050 Resin (right) Used for Composites

The fiber-matrix mixture is laid flat into a mold and pressed tight to eliminate any gaps and increase density. Pressure is applied by clamping the two mold surfaces together to ensure good bonding and removal of excess resin, as shown in Figure 6. At this point the wet layout is placed into a vacuum bag with bleeder cloth

and a vacuum is attached to the bag. The vacuum pulls the excess resin from the composite as the resin begins to cure, and the bleeder cloth absorbs this excess, protecting the vacuum.

The composite is allowed to cure in the oven at 40°C for six hours then removed from the mold where it finishes setting. Note that no vacuum was used for this project in order to obtain more consistent testing results and to achieve samples with repeatable properties such as volume fraction and total mass. Figure 7 contains kenaf fiber-reinforced composite samples created using this method along with a neat resin sample created in the same mold.

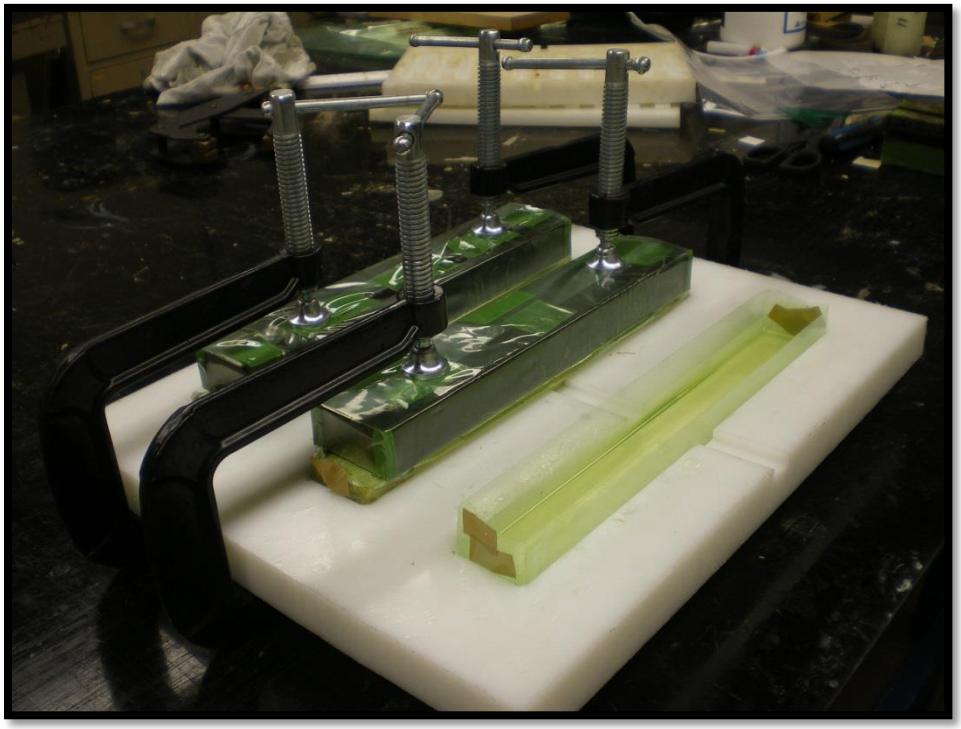

Figure 6: Mixed Fibers and Resin Clamped into the Mold Prior to Curing

Figure 7: Cured Kenaf Fiber-Reinforced Composites and a Neat Epoxy Sample

4.2 Overview of the Testing Method

In order to obtain the required damping properties, an impact hammer and accelerometer are employed. A dynamic signal analyzer (DSA) acquires the vibrational response from the accelerometer and transfers that data to a computer for further analysis of the vibrations. This approach has been used frequently to test a variety of materials including other composite materials [3],[34]. It provides a

quick, accurate method for obtaining damping characteristics of a material with limited required equipment. By implementing this procedure to kenaf-reinforced composite structures, damping data can be acquired for the biofibers. The test setup and method is further described in the succeeding sections.

4.3 Description of Test Setup

Damping properties can be effectively and soundly measured through use of an impact hammer and accelerometer. This method has been used in published research to test other materials including composites. The test setup is represented in Figure 8 and photographed in Figure 9.

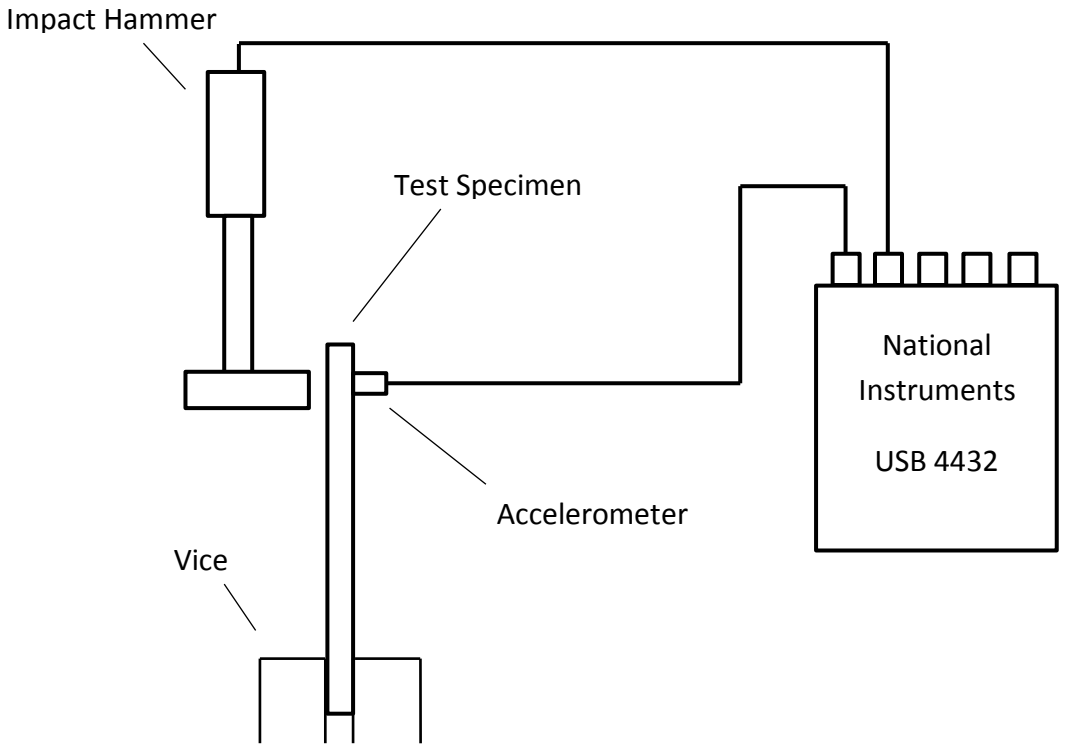

Figure 8: Depiction of the Vibrational Test Setup

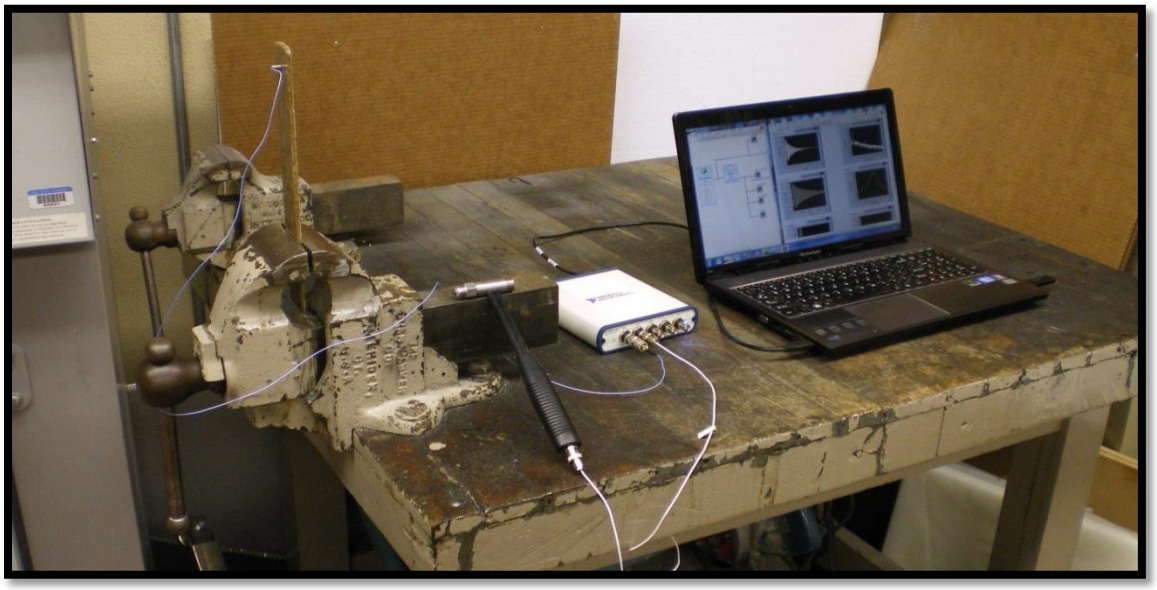

Figure 9: Photograph of the Vibrational Test Setup

The specimen is clamped on one end creating a fixed-free boundary condition set, with an accelerometer attached to the free end. The free end is struck with the impact hammer to initiate the free vibrations. Both the accelerometer and the impact hammer are connected to a dynamic signal analyzer (National Instruments USB-4432) that converts the signal from analog to digital. This vibrational data signal is collected at 4096 Hz for two seconds using a LabVIEW Virtual Instrument (VI) shown in Figure 10.

The LabVIEW VI records the acceleration measurements on a time domain and transforms them into a frequency domain through a Fast Fourier Transform (FFT). LabVIEW plots the response on a frequency domain from which the damping properties of the material are determined from the peak and half-power amplitudes and their corresponding frequencies using the half-power bandwidth method.

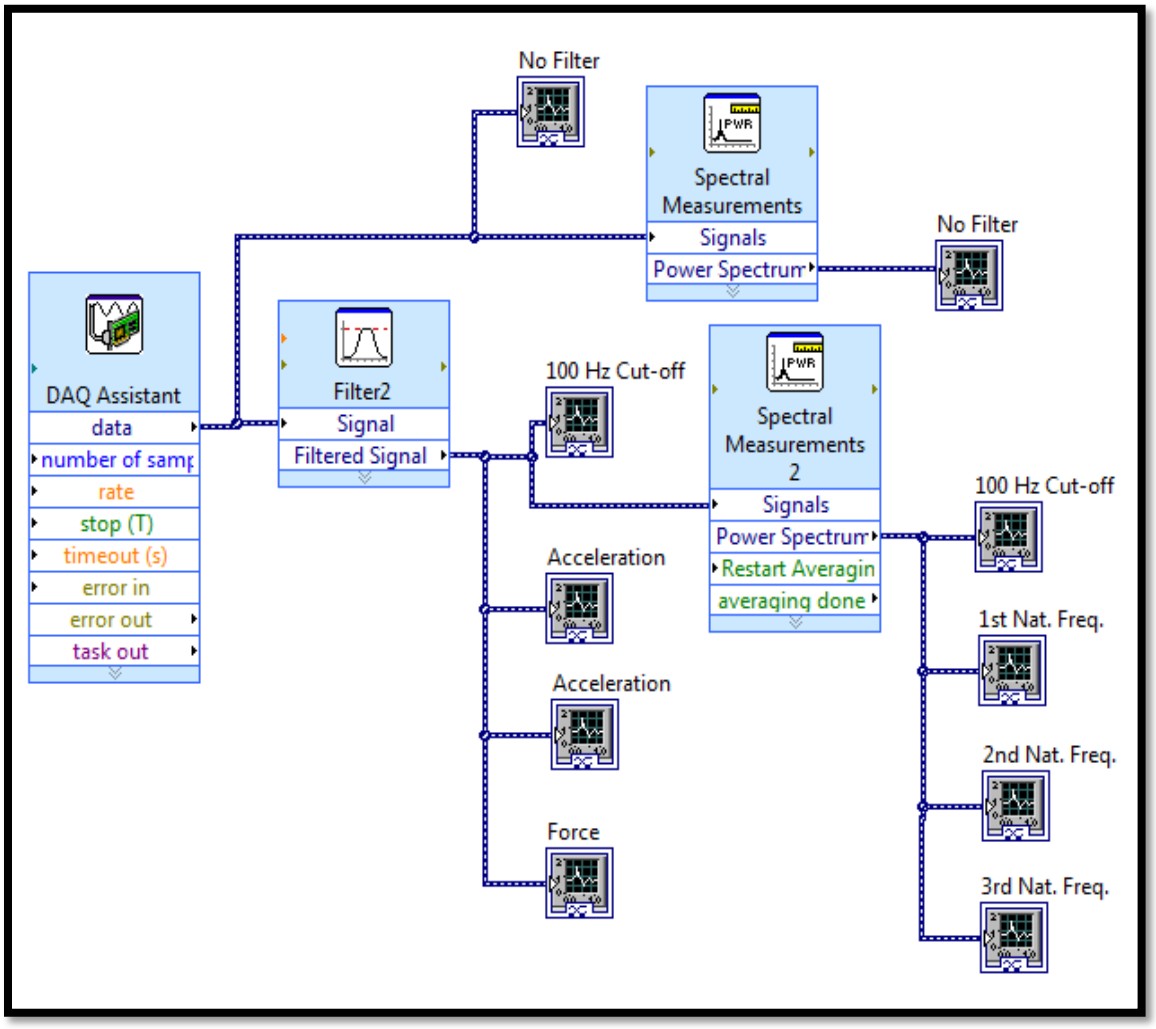

Figure 10: LabVIEW Block Diagram for Collecting Data and Performing the FFT

4.4 Half-Power Bandwidth Method

4.4.1 Obtaining Loss Factor from Response

The half-power bandwidth method allows for experimental measuring of the loss factor associated with damping. Obtaining a Frequency Response Function (FRF) is the first step, which was accomplished by using a FFT to convert the time

domain response into the frequency domain in the LabVIEW VI. This yields a plot of power magnitude in decibels (dB) as a function of frequency in Hertz (Hz) [24],[35].

The loss factor, η, describes the energy dissipated per cycle of deformation [22]. The loss factor is derived and its use is justified in ensuing paragraphs. The result of interest is the loss factor

$$\eta = \frac{\omega_2 - \omega_1}{\omega_n} \tag{4.1}$$

defined by the natural frequency of the system, ω_n, and two other frequencies, ω_1 and ω_2, located at positions 3.01 dB below the peak amplitude. This method derives its name from the requirement that the additional two frequencies correspond to points at half of the peak power, that is, at a voltage of $\frac{1}{\sqrt{2}}$ times the peak voltage or 3.01 dB below the maximum amplitude. Therefore, ω_1 and ω_2 can be found on the horizontal line located 3.01 dB below the peak value on the FFT plot. The difference between these frequencies is known as the bandwidth as shown in Figure 11.

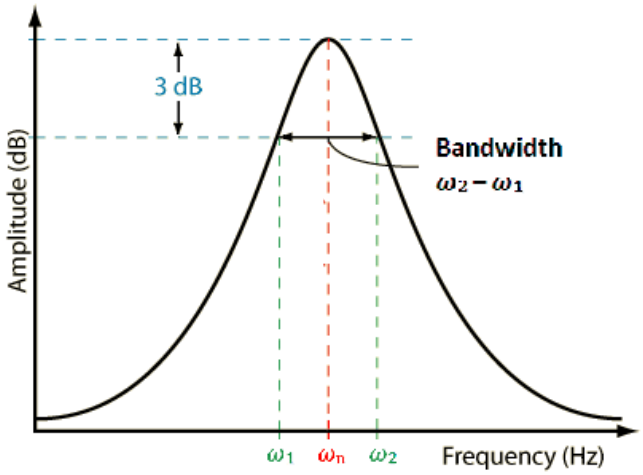

Figure 11: Half-Power Bandwidth Method for Frequency Domain Response

This method is often used in conjunction with impact testing and will be used for the composite specimens in this report. Modeling the setup as a viscoelastic system depicts the system as a mass attached to a spring and damper as shown in Figure 12.

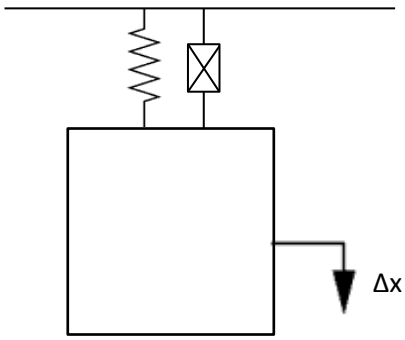

Figure 12: Composite Represented as a Spring-Mass-Damper System

4.4.2 Derivation of the Loss Factor

The continuous composite material sample can be approximated by such a discrete system. The motion of this system is described by the equation of motion

$$m\ddot{x} + kx = 0 \tag{4.2}$$

where m is the mass of the composite, k is the stiffness, and x and $\ddot{x}$ are the displacement and acceleration respectively. The stiffness is defined by a complex stiffness which accounts for the damping in the system.

$$k = k_r + ik_i = k_r(1 + i\eta) \tag{4.3}$$

Here k_r is the real stiffness and k_i is the imaginary stiffness being related by $i = \sqrt{-1}$ and the loss factor, η. Combining these two equations leaves the single degree of freedom (DOF) equation of motion for free vibration

$$m\ddot{x} + k_r(1 + i\eta)x = 0. \tag{4.4}$$

The loss factor is obtained experimentally by subjecting the specimen to a forcing function. This is supplied by an impact hammer, which can be represented by

$$F(\omega, t) = Re[Fe^{i\omega t}] \tag{4.5}$$

where Re denotes the real part of the forcing term in brackets, ω is the frequency, and t is the time. The equation of motion due to the forcing function is written as

$$m\ddot{x} + k_r(1 + i\eta)x = Re[Fe^{i\omega t}]. \tag{4.6}$$

Determining the steady-state solution to this differential problem yields

$$x = Xcos(\omega t + \alpha) \tag{4.7}$$

where X is the amplitude of x, defined by

$$X = \frac{F}{\sqrt{(k - m\omega^2)^2 + k^2\eta^2}} \tag{4.8}$$

and has a maximum value of

$$X_{max} = \frac{F}{k\eta} \tag{4.9}$$

when the frequency equals the resonance frequency.

$$\omega_n = \sqrt{\frac{k}{m}} \tag{4.10}$$

The half-bandwidth method requires two frequencies which are located at an amplitude 3.01 dB below the peak, or equivalently, at a factor of $\frac{1}{\sqrt{2}}$ times the peak. This means

$$\frac{1}{\sqrt{2}}\frac{F}{k\eta} = \frac{F}{\sqrt{(k - m\omega^2)^2 + k^2\eta^2}}. \tag{4.11}$$

The desired frequencies can be determined by solving this equation. The results are

$$\omega_1 = \sqrt{\frac{k(1+\eta)}{m}} \tag{4.12}$$

and

$$\omega_2 = \sqrt{\frac{k(1-\eta)}{m}}. \tag{4.13}$$

From these two frequencies along with the natural frequency from equation 4.10, the following relationship can be formulated.

$$\frac{\omega_2-\omega_1}{\omega_n} = \sqrt{1+\eta} - \sqrt{1-\eta} \tag{4.14}$$

This is not the exact relation expected. Recall from equation 4.1 that the following relationship was assumed for the frequencies and loss factor.

$$\eta = \frac{\omega_2-\omega_1}{\omega_n} \tag{4.15}$$

While the mathematical result does not exactly meet this assumption, it is approximately the same for small loss factors. This means that

$$\eta \approx \frac{\omega_2-\omega_1}{\omega_n} = \sqrt{1+\eta} - \sqrt{1-\eta}. \tag{4.16}$$

4.4.3 Justification of Simplified Equation

Table 4 is obtained by inserting different nominal values into the η terms on the right hand side of equation 4.16 and finding the calculated η on the left hand side. These nominal and calculated loss factors are tabulated below along with the relative difference between the two. The difference is defined as

$$\frac{|\eta_{calc}-\eta_{nom}|}{\eta_{nom}} * 100. \tag{4.17}$$

Table 4: Comparison of Two Loss Factor Calculations

Nominal Loss Factor	Calculated Loss Factor	Difference
0.0000	0.0000	0.0%
0.1000	0.1001	0.1%
0.2000	0.2010	0.5%
0.3000	0.3035	1.2%
0.4000	0.4086	2.2%
0.5000	0.5176	3.5%
0.6000	0.6325	5.4%
0.7000	0.7561	8.0%

Table 4 shows that for high loss factors, the accuracy of this simplified equation begins to fail. However, it is accurate to within half of one percent for values up to two-tenths. In this project, the loss factor remains below one-tenth, corresponding to one-tenth of a percent difference from the actual value. Therefore, the relationship used in this report is

$$\eta \approx \frac{\omega_2 - \omega_1}{\omega_n}. \tag{4.18}$$

4.5 Multiple Mode Shapes

A continuous system such as this one has an infinite number of mode shapes. This means that a vibration test results in the excitation of several frequencies each corresponding to a different mode. The first three mode shapes are represented in Figure 13. Each corresponds to a different natural frequency, and appears on the frequency domain response plot as a peak at that frequency. For this test the first

peak is analyzed to obtain the loss factor since it is the largest and most well defined. Therefore it yields the most accurate and repeatable results.

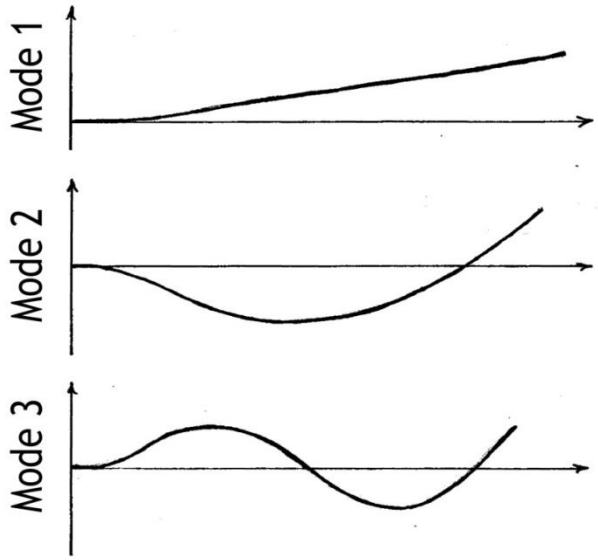

Figure 13: First Three Vibrational Modes for a Fixed-Free Beam

CHAPTER 5

RESULTS AND DISCUSSION

5.1 Stainless Steel

The method described was verified using a stainless steel sample since all parameters of interest are well established and/or testable. A stainless steel sample 1 mm thick, 25 mm wide, with a 200 mm overhang was clamped into a vice with an accelerometer attached to the free end. The specimen was impacted with the hammer and the vibrational response was recorded. Figure 15 shows the response to impact on the frequency domain. The peaks associated with the first three modes of vibration occur at 17.0 Hz, 111.5 Hz, and 316.0 Hz. The following equation is presented in "Mechanical Vibrations" for calculating the natural frequency of a beam

$$\omega_n = (\beta_n l)^2 \sqrt{\frac{EI}{\rho A l^4}} \tag{5.1}$$

where n is the mode number of interest, $\beta_n l$ is a set of constants describing the boundary conditions and mode of vibration (the first three for fixed-free boundary conditions are 1.8751, 4.6941, and 7.8548), E is the tensile modulus, l is the moment of inertia, ρ is the density, and A is the cross sectional area. Calculating these parameters and implementing them into the formulas yields the first three peak locations. According to equation 5.1 these peaks should exist at 19.4 Hz, 121.3 Hz, and 339.5 Hz. Table 5 shows the predicted and measured natural frequencies along with the percent error.

Table 5: Comparison of Calculated Natural Frequencies to Experimental Values for a Stainless Steel Specimen

Mode Number	Calculated Value	Experimental Value	Difference
1	19.4 Hz	17.0 Hz	12%
2	121.3 Hz	111.5 Hz	8%
3	339.5 Hz	316.0 Hz	7%

The table shows approximately a ten percent error between each predicted and corresponding measured frequency. The discrepancy is most likely due to the tensile modulus and density of the stainless specimen used. An average modulus and density for stainless steel were used for calculations. Differences may also be attributed to slight variances in specimen geometry from exactly prismatic. Even a small change in the sample thickness results in a large difference in the calculated natural frequency. However, despite the discrepancies, there exists a good, consistent correlation between the calculated and experimentally measured natural frequencies, which verifies that the LabVIEW VI is reading accurate data and correctly applying the FFT to create the FRF.

The output plots from the LabVIEW VI are shown below. Figure 14 shows the vibrational response on the time domain, Figure 15 shows the response on the frequency domain, and Figure 16 shows a closer view of the first peak in the frequency domain plot. This peak closely resembles the shape of the peak depicted in the model peak of Figure 11.

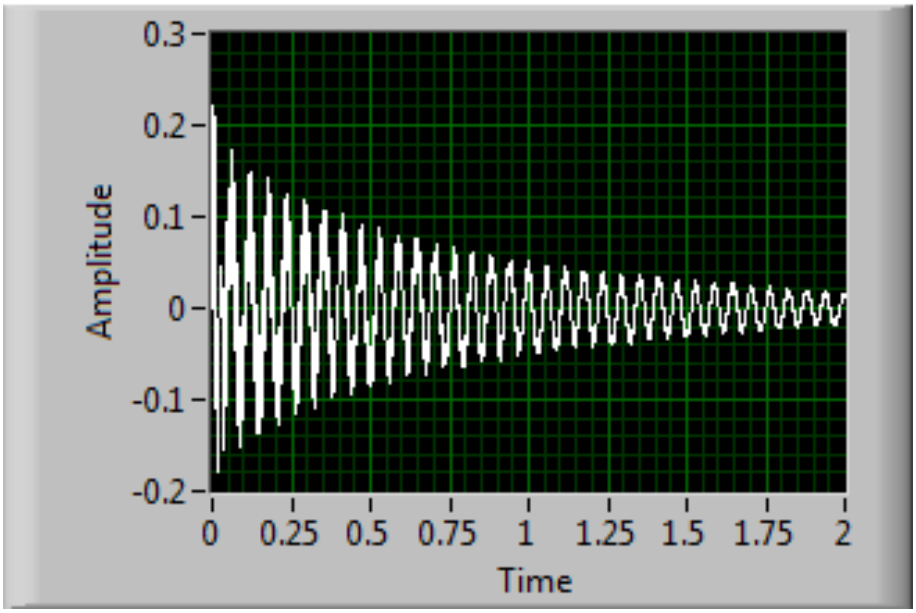

Figure 14: Time Domain Response of Stainless Steel Specimen

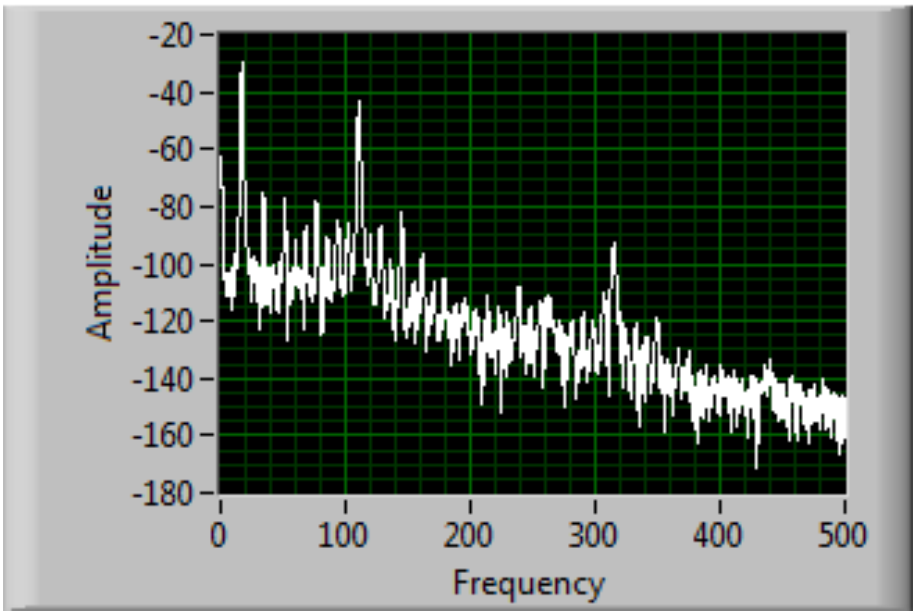

Figure 15: Frequency Domain Response of Stainless Steel Specimen

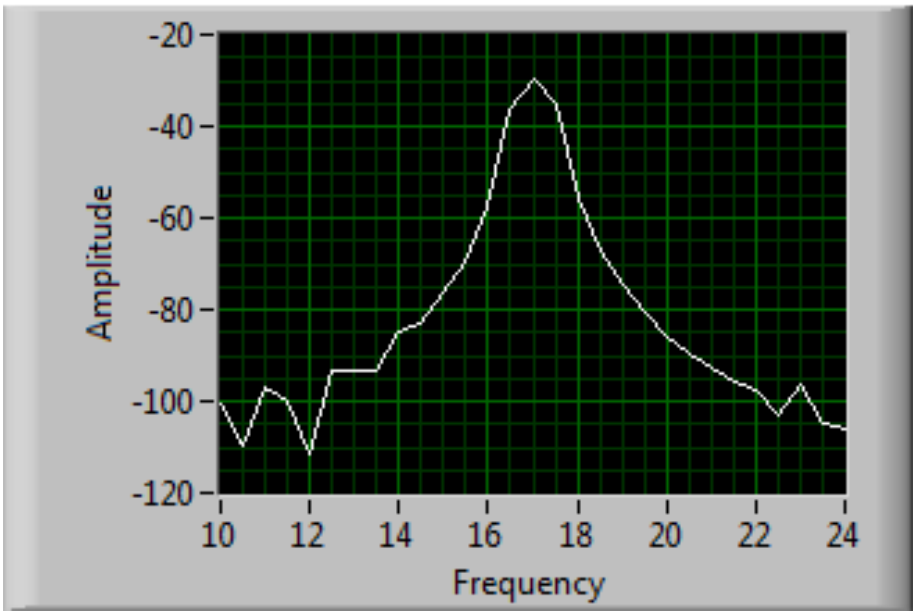

Figure 16: First Peak of Response for Stainless Steel Specimen

Colakoglu and Jerina [36] performed a similar vibrational test on stainless steel samples utilizing the half-power bandwidth method. However, they used an axial mode test with free-free boundary conditions instead of the transverse mode test with fixed-free boundaries used for this report. They report a damping factor of 0.0044, corresponding to a loss factor of 0.0088. Testing for this research yields a loss factor of 0.0156, nearly double the reported value. In stainless steel, the hysteretic damping is very low, so viscous damping has the ability to distort the result easily, especially in the transverse vibration tested in this research. It appears that approximately half of the damping for this sample is due to viscous damping in the air. For polymeric materials, the hysteretic damping is much higher, so viscous damping has less impact on the result of testing a composite specimen. This fact makes it less feasible to compare loss factor values from this report to

other research, but comparing test values to each other within this report is still very reliable. Viscous damping is very dependent on the shape and size of a sample, so its contribution will be consistent across all samples with the same dimensions.

5.2 Neat Epoxy

The test was also validated using a sample of neat epoxy 11 mm thick, 30 mm wide, and 200 mm long. This specific epoxy has a very high damping ability, much higher than stainless steel so the vibrations diminished much faster. Using the same method, the natural frequency was measured at 30.0 Hz with half power frequencies of 28.3 Hz and 31.4 Hz. These frequencies offer a damping loss factor of 0.103, nearly an order of magnitude higher than that of stainless steel. The damping loss factor for the epoxy material was expected to be much higher than for the stainless steel due to its polymeric makeup, and based on observation, which helps validate the test setup and methodology.

5.3 Repeatability of the Method

Three samples were repeatedly tested in a short time period to check the repeatability of this method. Samples A5, A18, and A24 were subjected to the vibrational test and the half-power bandwidth method was implemented to calculate the loss factor. Each specimen was tested eight times within an hour period to determine whether the test yielded consistent results over multiple trials. The results shown in Figure 17 contain little variance over the eight tests proving this a sound, repeatable method for determining the loss factor.

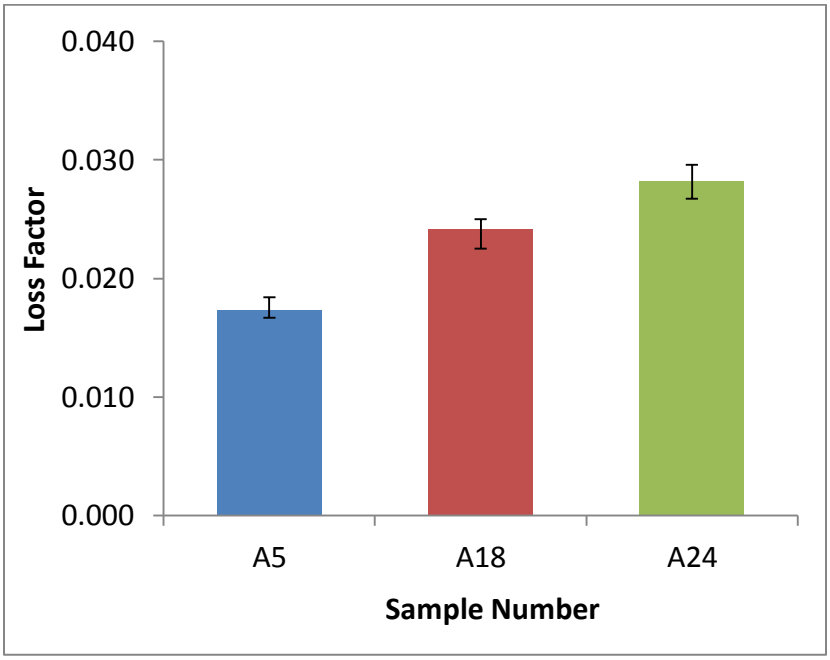

Figure 17: Average Loss Factor and Maximum Deviation over Eight Trials

5.4 Effect of Manufacturing Procedures

5.4.1 Effect of Varying Cure Time

The composites produced for this project were cured at 40°C for six hours then removed from the mold. These samples were tested between one and seven days after removal. When retested, nearly every sample exhibited a higher natural frequency and lower loss factor than when originally tested. The second round of testing also showed more consistent results. Despite appearing to be cured, the samples continue to set and cross-link, becoming more brittle over time. The average loss factor of each sample for the first and second set of tests is shown in Figure 18.

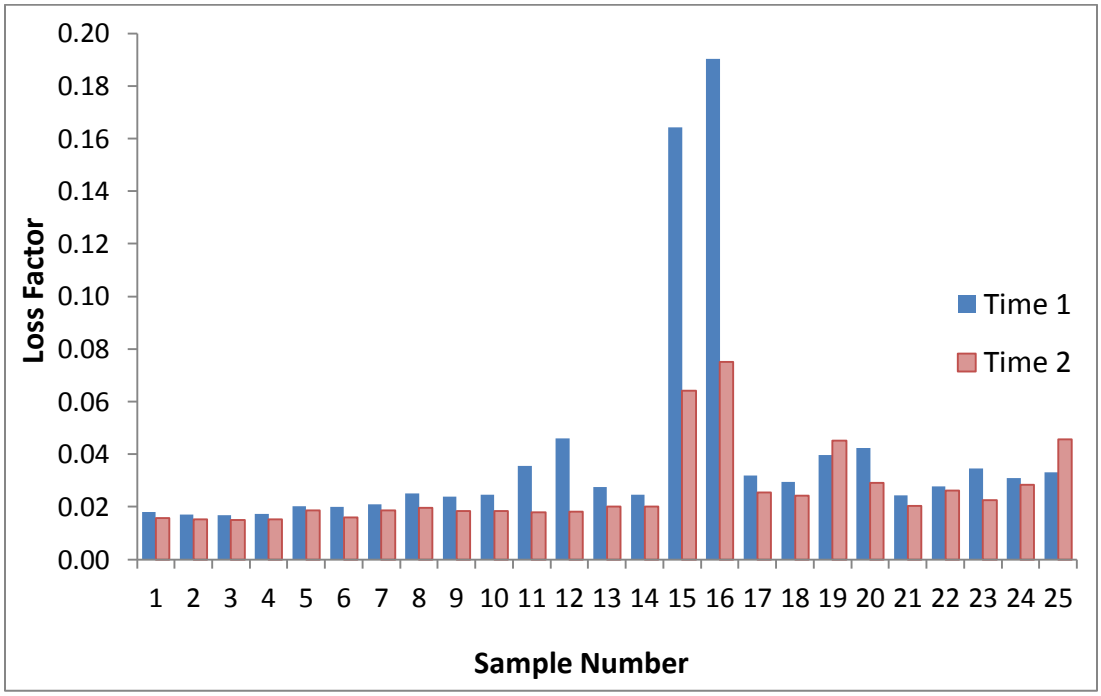

Figure 18: Change in Loss Factor over Time

When this was realized, two more samples were created and tested at known times to examine how time affects these parameters. Figure 19 and Figure 20 contain the results, showing that after 150 hours the loss factor and natural frequency stop changing. Therefore, it is suggested that samples be left for at least this long before testing them in order to avoid testing before the properties are set. Testing before the samples are set will result in spurious results with large inconsistencies that may mask actual trends and good conclusions. All samples in this research were tested later than the 150 hours required to ensure accurate results. These results are listed in Appendix A for reference.

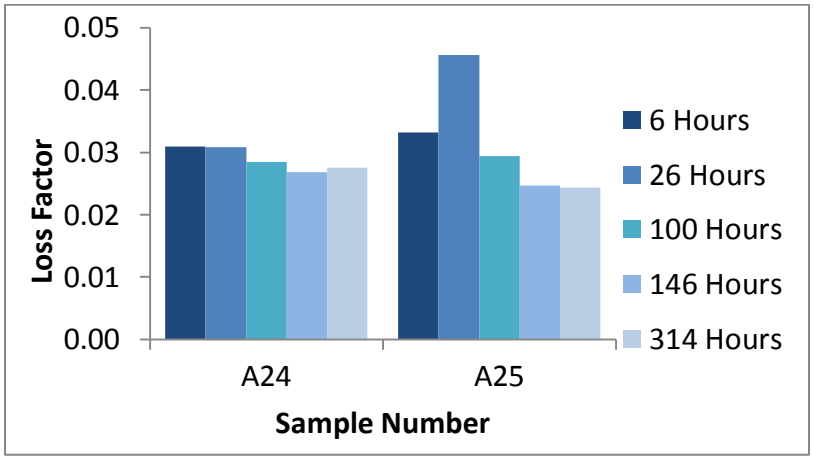

Figure 19: Loss Factor at Several Times after Removal from the Oven

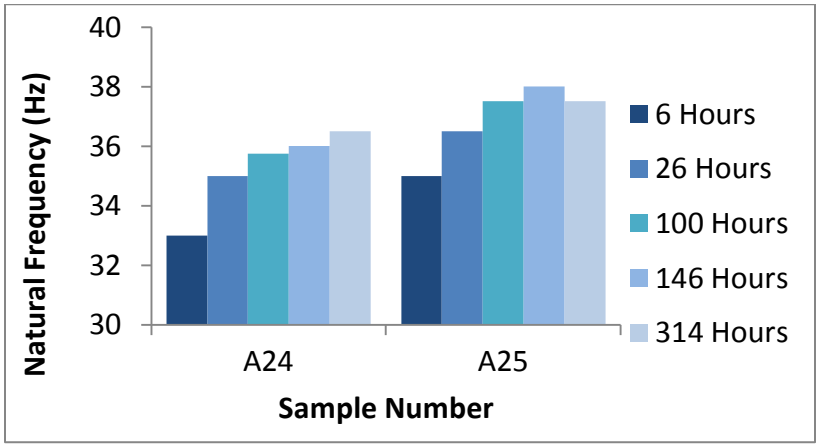

Figure 20: Natural Frequency at Several Times after Removal from the Oven

5.4.2 Effect of Varying Density

The density of the sample can be altered by changing the amount of pressure applied to the sample during the cure cycle. Low pressures could be applied using weights, but c-clamps were required to achieve higher pressures and densities. The density of the sample has a major influence on several other material properties as shown in Figure 21.

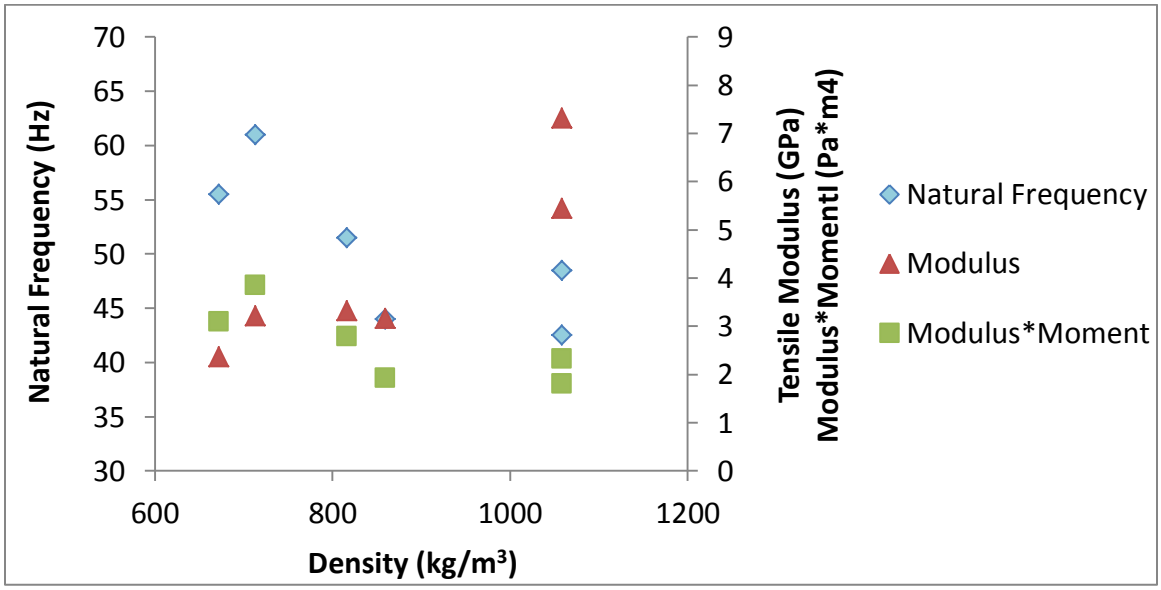

Figure 21: Effect of Density on Natural Frequency, Tensile Modulus, and the Product of Modulus with Moment of Inertia for Samples A1-A6

Samples were created and tested at densities ranging from 700 to 1200 kg/m^3, and the results are shown in Figure 22. This figure contains linear fits for the data, though the relationship is likely non-linear and there is insufficient data to verify the order of the relationship. The fit merely allows easy viewing of general trends. As the density increases, the tensile modulus does as well since the material is more tightly packed allowing for more cross-linking in the matrix and better bonding between the fibers and matrix. Most applications prefer a high amount of stiffness to provide rigidity. The natural frequency of a high density sample is lower than in a sample with low density. Recall that the natural frequency depends on both the density and the tensile modulus according to the following equation.

$$\omega_n = (\beta_n l)^2 \sqrt{\frac{EI}{\rho A l^4}} \qquad (5.2)$$

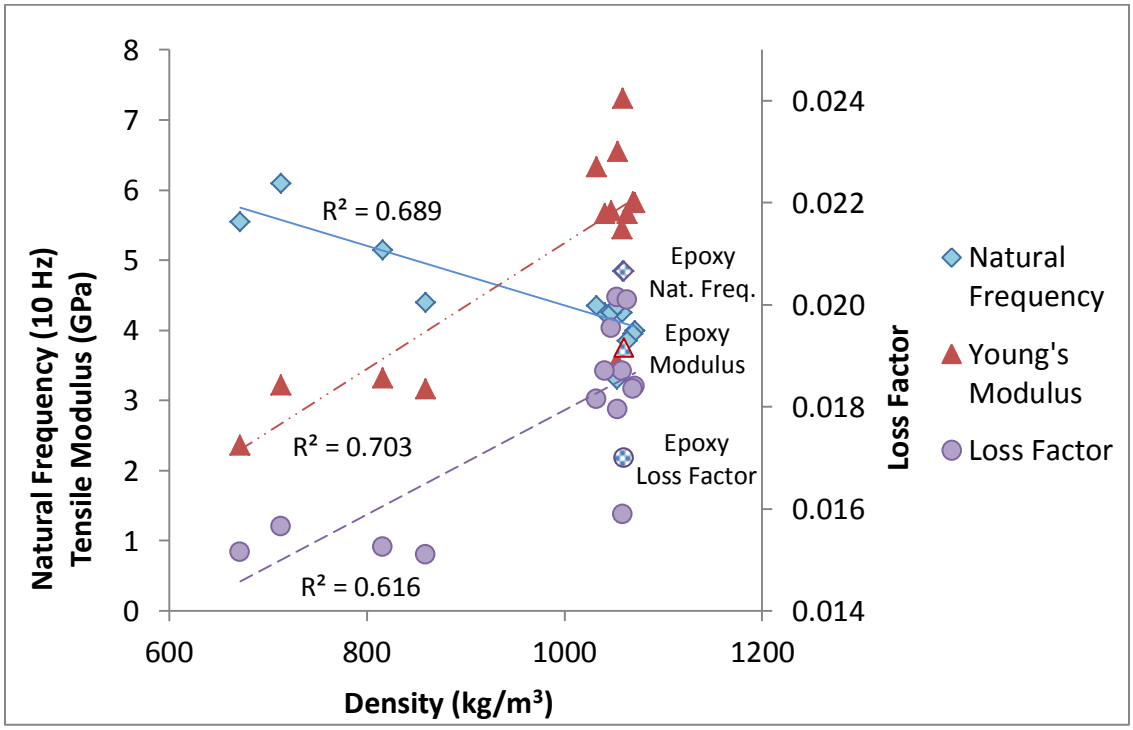

Figure 22: Effect of Density on Natural Frequency, Tensile Modulus, and Loss Factor for Samples A1-A14 (Solid Markers) and Neat Epoxy (Checker Markers)

The modulus actually increases faster than the density, but its product with the moment of inertia decreases with increased density resulting in a net decrease in natural frequency. The loss factor also increases with the density. A neat epoxy sample is also plotted in Figure 22 to compare its properties with the composite properties. The neat epoxy has a similar density to the high density samples but with less favorable properties including a lower loss factor and tensile modulus. Appendix B also contains bar graphs comparing the neat epoxy with composite samples grouped by density.

5.4.3 Effect of Varying Matrix Hardener Ratio

Changing the ratio of epoxy base to hardener may be another way to change the loss factor of a composite sample. Changing the ratio has an effect on several parameters, though the current testing showed the variation to be slight. The manufacturer's recommended ratio is 27:100 by weight. Samples were created using weight ratios of 24.5, 25, 26, 27, and 29:100, yielding the results in Figure 23.

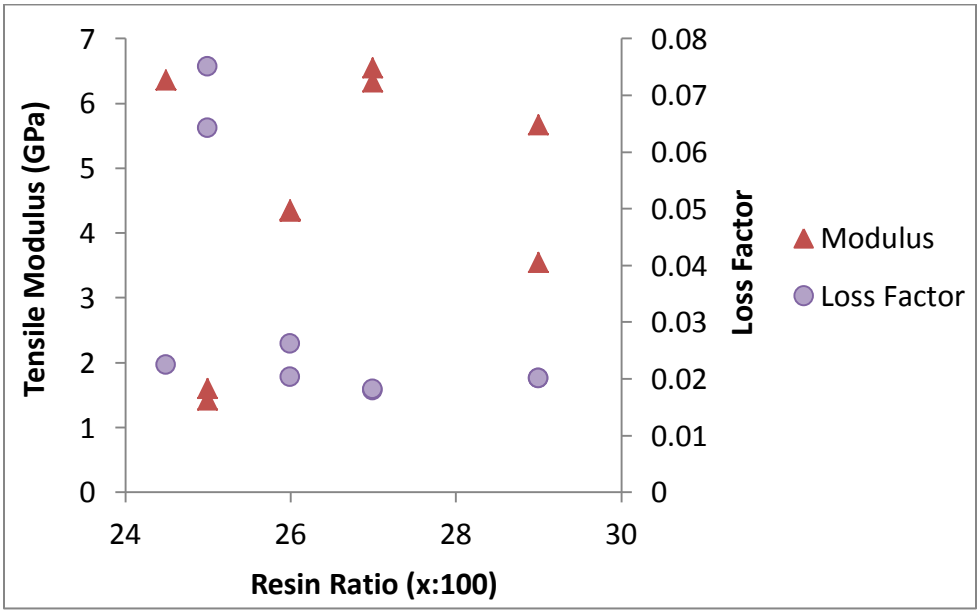

Figure 23: Effect of Resin Hardener Ratio on Tensile Modulus and Loss Factor

At low ratios, the neat epoxy is more pliable than at higher ratios, leading to a higher loss factor, which tends to decrease with higher hardener ratios. In fact, some of the neat epoxy samples at the lowest ratios were very pliable such that they could be bent and manipulated easily. The equivalent samples that contained fibers inside were much more rigid making it clear that the fibers caused greater stiffness.

The fibers have a higher stiffness than the matrix at the recommended ratio, making most composites more rigid than their neat epoxy equivalent that contains no fibers, but at low ratios it is very easy to feel the difference as well as test for it. On the other extreme is the 29:100 ratio, which became so brittle that the neat epoxy sample cracked when placed in the vice. Therefore, this sample could not be tested. However, the composites made from this had no such problem suggesting that the fibers added some compliance to the sample at such a high ratio.

Because the samples with a low hardener ratio are more pliable, they dampen the vibrations better, but have a lower tensile modulus. The composite sample with the highest modulus was found for the samples at the recommended weight ratio of 27:100. This is expected since the majority of testing is done with strength and stiffness in mind and recommendations are given to maximize these properties. However, there are applications where damping characteristics become more essential than the stiffness. Therefore this ratio may not be the best for all applications since the stiffness was high at the recommended ratio but the loss factor was lower than in the other samples.

Damping in a composite material depends on the matrix properties and the fiber properties, but it is also determined by the relative stiffness of the two. A greater difference between the fiber stiffness and matrix stiffness leads to one component elongating or bending more than the other in the presence of a load. This develops shear in the composite upon vibration or load cycling and results in loss of energy.

One set of samples, created at a 25:100 ratio, had very extreme parameters, proving to be an outlier in most of the tested properties. This sample was easily manipulated and would even sag under its own weight. After further inspection it was realized that it did not set up well and had areas that remained tacky. This indicates that the epoxy did not get mixed together thoroughly causing sections to set up slowly or not at all. These sections definitely influenced the results, making it a poor candidate for comparing hardener ratios, but indicating the importance of mixing the resin thoroughly and completely.

5.4.4 Effect of Varying Fiber Surface Treatment

The effect of surface treatments on damping characteristics was tested by soaking fibers in a sodium hydroxide (NaOH) solution. The first set of fibers were untreated, the second set were exposed to a 3% NaOH solution for 30 minutes, the third set of fibers to a 5% NaOH solution for 60 minutes, and the fourth set exposed to an 8% solution for 75 minutes. Samples subjected to each chemical treatment underwent a vibrational test to determine the effect of each treatment on the loss factor. Figure 24 indicates that samples which were treated generally had a higher loss factor than those which were not treated. This outcome is counter to expected results. Exposure to such a chemical was predicted to make a sample dampen less because the fibers and matrix are better bonded together allowing for less sliding and shifting between the two in the interphase region. Test results show the opposite to be true, that chemically treated fibers lead to a higher loss factor.

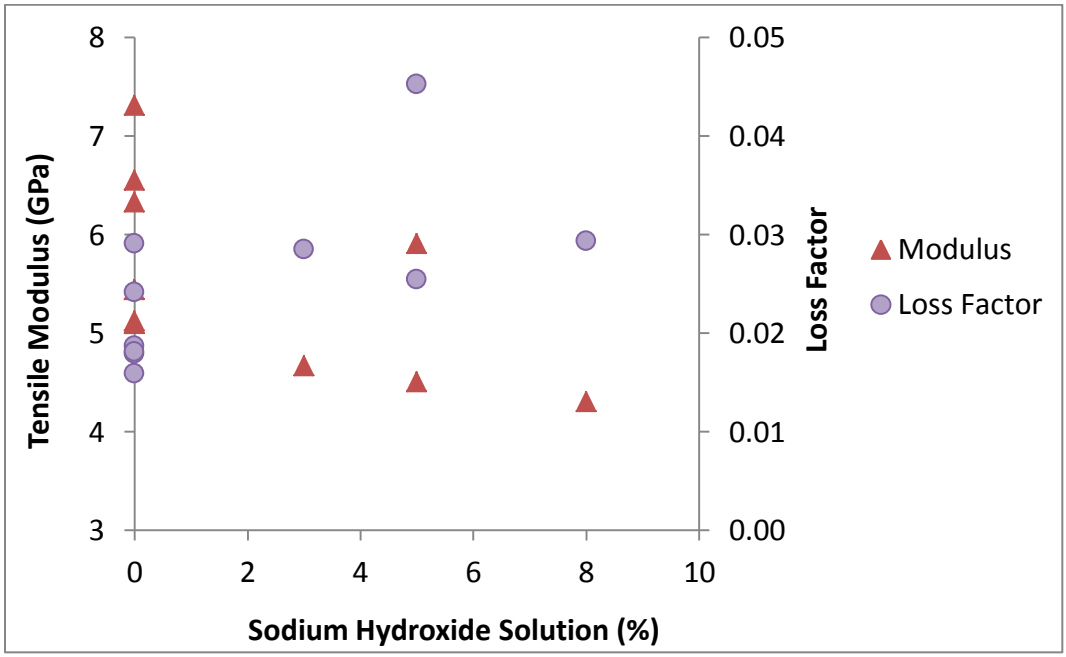

Figure 24: Effect of Surface Treatment on Tensile Modulus and Loss Factor

5.4.5 Effect of Varying Fiber Length

Many papers and texts suggest that the fiber length has a slight influence on the damping characteristics associated with a created sample. Samples were made out of fibers ranging from 5 mm to 80 mm in length. Testing done here does not suggest that fiber length has a significant impact, which agrees with calculations. In the sensitivity analysis performed, changing the fiber length had a very insignificant impact on the overall loss factor. Appendix C shows the statistical significance of each parameter calculated using the code included in Appendix D. The fiber length has very little influence on the loss factor. Therefore, the effect of changing fiber length is hidden by incidental variance in other properties from one sample to

another. The effect of fiber length is likely more pronounced in very short fiber composites if they remain shorter than the 10 mm optimal fiber length.

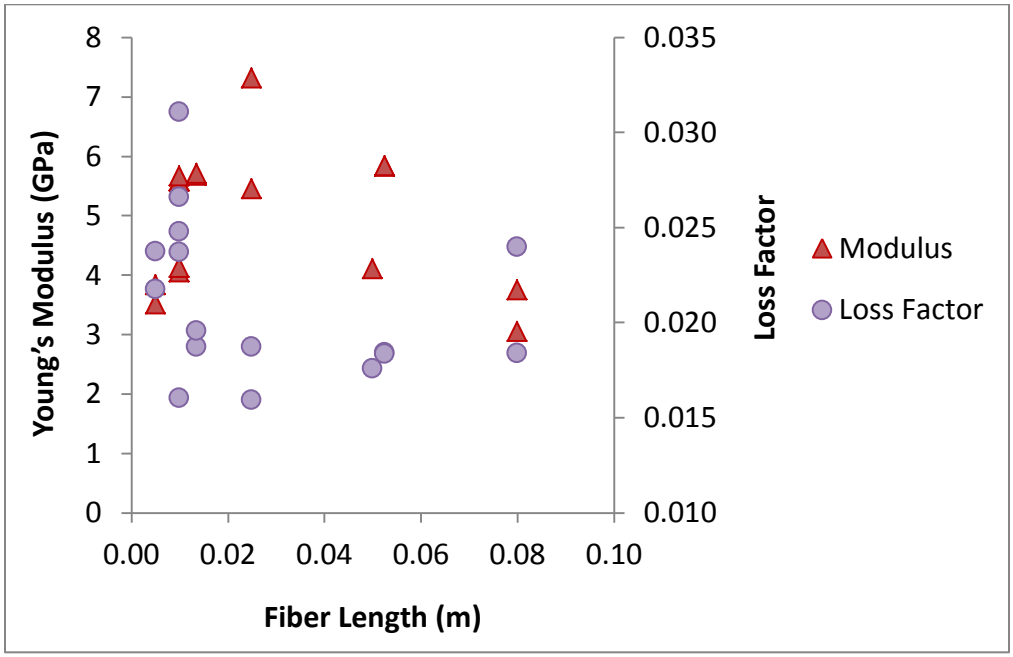

Figure 25: Effect of Fiber Length on Tensile Modulus and Loss Factor

CHAPTER 6

CONCLUSIONS

This paper examines the effect of various manufacturing parameters of kenaf fiber-reinforced composites including cure time, density, matrix hardener ratio, surface treatment, and fiber length on the mechanical properties of the composite material such as natural frequency, damping loss factor, and tensile modulus. Researchers are beginning to examine many of these significant properties, but results vary and the models built to predict the mechanical properties of these composites contain extensive differences [22],[27]. Use of an impact hammer and accelerometer accompanied by a LabVIEW VI and the developed half-power bandwidth method allow for the determination of these properties from a vibrational test. The factors that are tested for their influence on damping include the cure time, the density of the sample, the matrix hardener ratio, the chemical treatment of fibers, and the fiber length.

The research aims to determine how these manufacturing procedures influence the composite properties, but also intends to find what influence they have on the interphase region specifically. The interphase is predicted to contribute to the mechanical properties of the composite, though its specific properties and actual influence are not well known. Finding the influence of the interphase is a very challenging task because this region cannot be tested directly and such properties are difficult to infer from indirect tests. The properties are influenced by

a multitude of attributes, each difficult to isolate. Viscous damping intermingles with the material damping causing trouble in finding reliable loss factors. Also, very slight variances in certain properties have more influence than large adjustments to other properties making it hard to isolate a single input and analyze its effect on the composite's properties. The equations for calculating the loss factor become very complicated requiring inputs that are not directly measurable. For these reasons, finding mechanical properties of the interphase and its influence on the composite is difficult. However, a method for determining the interphase loss factor is derived (see equation 3.10), providing a glimpse into the effect of interphase on damping and offering an area for further work. This research could be accomplished using a Dynamic Mechanical Analysis device to measure the complex moduli of the matrix and composite to find the isolated interphase loss factor.

Samples which are oven-cured for six hours at 40 °C exhibit repeatable mechanical properties approximately 150 hours following removal. When creating samples it is important to ensure the specimen has fully cured before testing it. Even after the sample appears to be cured, the mechanical properties are continually changing due to ongoing cross-linking in the matrix. Testing prior to final cure will lead to inconsistent and spurious results that may mask true results and trends.

Increasing the pressure applied during the cure cycle results in higher densities, loss factors and tensile moduli, along with lower natural frequencies. High density samples promote a better bond between the fiber and matrix as well as

more cross-linking in the matrix, which result in higher strength and stiffness. The natural frequency is directly proportional to the stiffness, but inversely proportional to the density, creating a battle between the two when they both increase (see equation 5.2). However, adding additional pressure decreases the thickness of the sample and therefore the moment of inertia. Considering all effects together, the addition of pressure is found to decrease the natural frequency. Applying good pressure during the manufacturing process provides the most simple and effective way to ensure strength, stiffness, and damping characteristics are optimized in the produced composite.

The matrix hardener ratio also affects these properties in a similar way and proves to be another effective way to affect the damping and stiffness of a composite. High hardener ratios result in a more brittle material that dampens less but generally has a higher stiffness. The peak stiffness occurred at the recommended weight ratio of 27:100. The actual peak damping would vary based on which fibers are used because damping depends not only on the stiffness of the fibers and matrix independently; it also depends on the relative stiffness between the two. As the specimen cycles due to loading or from vibrations the matrix and fibers elongate and bend. When the two stiffness values differ, shear develops between them resulting in cyclical material damping in the specimen. Therefore, if a different fiber or matrix material is used in testing, the optimal hardener ratio for maximum damping will likely change. This hypothesis provides opportunity for

interesting testing using different matrix resins as well as different fibers, both natural and synthetic.

The energy model examined [22] predicts that a chemical surface treatment would decrease the loss factor since the fiber and matrix would bond better, resulting in less sliding and friction. However, testing shows the opposite result with treated fibers exhibiting higher amounts of damping. When fibers are chemically treated, they do create a better bond with the matrix. However, chemical treatments can have negative effects on the fiber. The treatment etches away part of the fiber, altering the mechanical properties of the fibers, and resulting in lower strength and stiffness. This change in properties may also influence the damping characteristics of the sample.

Fiber length is also examined, though the results are not significantly different at the lengths tested. As discussed, shear forms between the fiber and matrix for cases where the respective stiffness values differ. This occurs along the fiber edges as well as at the ends of the fibers. Shorter fibers should mean more ends and therefore higher damping. However, the fibers have very small cross-sectional areas compared to their lengths. Therefore, to make a significant difference in damping, the fiber length has to change very dramatically and will play a larger roll if the fibers are very short. Kenaf fibers have inconsistent cross-sectional areas along the length of the fiber, leading to areas of higher and lower ultimate strength. The strength of the fiber is determined by the weakest point. For short fibers, a single weak point determines the strength. For longer fibers, several such points

exist offering the fiber no more strength or stiffness than the short fiber. Strength may be increased by using very short fibers since there is less length for weak points. Further examination of this point could verify this result in additional research.

This paper delves into the influence of composite cure time, sample density, matrix hardener ratio, fiber surface treatment, and fiber length and finds the influence each had on the stiffness and damping properties of a kenaf fiber-reinforced composite. It identifies sample density and matrix hardener as the most influential and feasible ways to affect the mechanical properties of the composite. A method for testing these parameters and calculating the required properties is successfully developed. Current research recognizes kenaf as a natural fiber with potential to replace glass fibers [1],[21], while this research produces information regarding the damping and stiffness characteristics of kenaf fiber-reinforced composites. Kenaf has similar specific stiffness and strength compared to glass fibers and has favorable damping characteristics, while being more environmentally friendly and potentially cost-competitive.

REFERENCES

[1] Akil, H. M., Omar, M. F., Mazuki, A. A. M., Safiee, S., Ishak, Z. A. M., and Bakar, A. A., "Kenaf Fiber Reinforced Composites: A Review," *Materials & Design*, Vol. 32, No. 8-9, 2011, pp. 4107-4121.

[2] Shibata, S., Cao, Y., and Fukumoto, I., "Lightweight Laminate Composites Made from Kenaf and Polypropylene Fibres," *Polymer Testing*, Vol. 25, No. 2, 2006, pp. 142-148.

[3] Etaati, A., Mehdizadeh, S. A., Wang, H., and Pather, S., "Vibration Damping Characteristics of Short Hemp Fibre Thermoplastic Composites," *Journal of Reniforced Plastics and Composites*, Vol. 33, No. 4, 2014, pp. 330-341.

[4] Bledzki, A. K., and Gassan, J., 1999, "Composites Reinforced with Cellulose Based Fibres," *Progress in Polymer Science*, Vol. 24, No. 2, 1999, pp. 221-274.

[5] Davoodi, M. M., Sapuan S. M., Ahmad, D., Ali, A., Khalina, A., and Jonoobi, M., "Mechanical Properties of Hybrid Kenaf/Glass Reinforced Epoxy Composite for Passenger Car Bumper Beam," *Materials & Design*, Vol. 31, No. 10, 2010, pp. 4927-4932.

[6] Ashori, A., Ornelas, M., Sheshmani, S., and Cordeiro, N., "Influence Of Mild Alkaline Treatment On The Cellulosic Surface Active Sites," *Carbonhydrate Polymers*, Vol. 88, No. 4, 2012, pp. 1293-1298.

[7] Mohanty, A. K., Misra, M., and Drzal, L. T., "Natural Fibers, Biopolymers, and Biocomposites: An Introduction," *Natural Fibers, Biopolymers, and Biocomposites*, 1st ed., Taylor & Francis Group, LLC, Florida, 2005, pp. 6-12.

[8] Naishino, T., Hirao, K., Kotera, M., Nakamae, K., and Inagaki, H., "Kenaf Reinforced Biodegradable Composite," *Composites Science and Technology*, Vol. 63, No. 9, 2003, pp. 1281-1286.

[9] Anuar, H., Ahmad, S. H., Rasid, R., Ahmad, A., and Wan Busu, W. N., "Mechanical Properties and Dynamic Mechanical Analysis of Thermoplastic-Natural-Rubber-Reinforced Short Carbon Fiber and Kenaf Fiber Hybrid Composites," *Journal of Applied Polymer Science*, Vol. 107, No. 6, 2008, pp. 4043-4052.

[10] Ochi, S., "Mechanical Properties of Kenaf Fibers And Kenaf/PLA Composites," *Mechanics of Materials*, Vol. 40, No. 4-5, 2008, pp. 446-452.

[11] Webber, C. L., and Bledsoe, V. K., "Plant Maturity and Kenaf Yield Components," *Industrial Crops and Products,* Vol. 16, No. 2, 2002, pp. 81-88.

[12] Hyer, M. W., "Fiber-Reinforced Composite Materials," *Stress Analysis of Fiber-Reinforced Composite Materials*, 1st ed., WCB McGraw-Hill, Ohio, 1998, pp. 10-26.

[13] Jones, R. M., "Introduction to Composite Materials," *Mechanics of Composite Materials,* 2nd ed., Taylor & Francis, Inc., Pennsylvania, 1999, pp. 23-33.

[14] Tsai, S. W., and Hahn, H. T., "Micromechanics," *Introduction to Composite Materials*, 1st ed., Technomic Publishing Company, Inc., Pennsylvania, 1980, pp. 405-419.

[15] Shokrieh, M. M., and Safarabadi, M., "Three-Dimensional Analysis of Micro-Residual Stresses in Fibrous Composites Based on the Energy Method: A Study Including Interphase Effects," *Journal of Composite Materials*, Vol. 46, No. 6, 2012, pp. 727-735.

[16] Finegan, I. C., and Gibson, R. F., "Analytical Modeling of Damping at Micromechanical Level in Polymer Composites Reinforced with Coated Fibers," *Composites Science and Technology*, Vol. 60, No. 7, 2000, pp. 1077-1084.

[17] Paipetis, A., and Galiotis, C., "Effect of Fibre Sizing on the Stress Transfer Efficiency in Carbon/Epoxy Model Composites," *Composites Part A: Applied Science and Manufacturing*, Vol. 27, No. 9, 1996, pp. 755-767.

[18] Williams, G. I., and Wool, R. P., "Composites from Natural Fibers and Soy Oil Resins," *Applied Composite Materials*, Vol. 7, No. 5-6, 2000, pp. 421-432.

[19] Cordeiro, N., Gouveia, C., and John, M. J., "Investigation of Surface Properties of Physico-Chemically Modified Natural Fibres Using Inverse Gas Chromatography," *Industrial Crops and Products*, Vol. 33, No. 1, 2011, pp. 108-115.

[20] Li, X., Tabil, L. G., and Panigrahi, S., "Chemical Treatments of Natural Fiber for Use in Natural Fiber-Reinforced Composites: A Review," *Journal of Polymers and the Environment*, Vol. 15, No. 1, 2007, pp. 25-33.

[21] Wambua, P., Ivens, J., and Verpoest, I., "Natural Fibres: Can they Replace Glass in Fibre Reinforced Plastics?" *Composites Science, and Technology*, Vol. 63, No. 9, 2003, pp. 1259-1264.

[22] Sun, C. T., and Lu, Y. P., "Damping of Fiber-Reinforced Composite Materials," *Vibration Damping of Structural Elements*, 1st ed., Prentice Hall, Inc., New Jersey, 1995, pp. 146-151.

[23] Mohanty, A. K., Misra, M., and Hinrichsen, G., "Biofibres, Biodegradable Polymers and Biocomposites: An Overview," Macromolecular Materials and Engineering, Vol. 276-277, No. 1, 2000, pp. 1-24.

[24] Rao, S., "Continuous Systems," *Mechanical Vibrations,* 5th ed., Pearson Education, Inc., New Jersey, 2011, pp. 721-726.

[25] Henwood, D. J., "Approximating the Hysteretic Damping Matrix by a Viscous Matrix for Modelling in the Time Domain," *Journal of Sound and Vibration*, Vol. 254, No. 3, 2002, pp. 575-593.

[26] Yao, Y., Chen, S. H., and Chen, P. J., "The Effect of a Graded Interphase on the Mechanism of Stress Transfer in a Fiber-Reinforced Composite," *Mechanics of Materials*, Vol. 58, Mar., 2013, pp. 35-54.

[27] Chandra, R., Singh, S. P., and Gupta, K., "A Study of Damping in Fiber-Reinforced Composites," *Journal of Sound and Vibration*, Vol. 262, No. 3, 2003, pp. 475-496.

[28] Gohil, P. P., and Shaikh, A. A., "Analytical Investigation and Comparative Assessment of Interphase Influence on Elastic Behavior of Fiber Reinforced Composites," *Journal of Reinforced Plastics and Composites*, Vol. 29, No. 5, 2010, pp. 685-699.

[29] Nishino, T., Hirao, K., Kotera, M., Nakamae, K., and Inagaki, H., "Kenaf Reinforced Biodegradable Composite," Composites Science and Technology, Vol. 63, No. 9, 2003, pp. 1281-1286.

[30] McHugh, J., Döring, J., Stark, W., and Erhard, A., "Characterisation of Epoxy Materials used in the Development of Ultrasonic Arrays." *Proceedings of the 16th World Conference on Non-Destructive Testing*, 2004, Montreal, Canada.

[31] Gassan, J., and Bledzki, A. K., "Possibilities for Improving the Mechanical Properties of Jute/Epoxy Composites by Alkali Treatment of Fibres," *Composites Science and Technology*, Vol. 59, No. 9, 1999, pp. 1303-1309.

[32] Ibrahim, N. A., Hadithon, K. A., and Abdan, K., "Effect of Fiber Treatment on Mechanical Properties of Kenaf Fiber-Ecoflex Composites," *Journal of Reinforced Plastics and Composites*, Vol. 29, No. 14, 2010, pp. 2192-2198.

[33] Edeerozey, A. M. M., Akil, Hazizan Md A., Azhar, A. B., and Ariffin, M. I. Z., "Chemical Modification of Kenaf Fibers," *Materials Letters*, Vol. 61, No. 10, 2007, pp. 2023-2025.

[34] Fotsing, E. R., Sola, M., Ross, A., and Ruiz, E., "Lightweight Damping of Composite Sandwich Beams: Experimental Analysis," *Journal of Composite Materials*, Vol. 47, No. 12, 2012, pp. 1501-1511.

[35] Novascone, S. R., 1998, "The Effects of Manufactured Defects on the Axial Damping Characteristics of Composite Specimens," M.S. Thesis, Mechanical and Aerospace Engineering, Utah State University, 1998.

[36] Colakoglu, M., and Jerina, K. L., "Damping Behaviour of Cyclically Deformed 304 Stainless Steel." *Indian Journal of Engineering & Materials Sciences*, Vol. 10, Dec., 2003, pp. 480-485.

APPENDICES

Appendix A

Loss Factor Calculations

Table 6: Neat Epoxy Specimen (27:100, 1060 kg/m3)

Test #	ω_n	ω_1	ω_2	η
1	35.00	34.48	35.56	0.0309
2	35.00	34.49	35.73	0.0354
3	36.50	35.68	37.19	0.0414

Table 7: Sample A01 (25 mm, No Treatment, 27:100, 713 kg/m3)

Test #	ω_n	ω_1	ω_2	η
1	60.50	60.15	61.23	0.0179
2	61.00	60.24	61.36	0.0184
3	61.00	60.34	61.30	0.0157
4	61.00	60.39	61.34	0.0156

Table 8: Sample A02 (25 mm, No Treatment, 27:100, 672 kg/m3)

Test #	ω_n	ω_1	ω_2	η
1	55.00	54.70	55.66	0.0175
2	55.50	54.86	55.77	0.0164
3	55.50	54.82	55.68	0.0155
4	55.50	54.91	55.73	0.0148

Table 9: Sample A03 (25 mm, No Treatment, 27:100, 860 kg/m3)

Test #	ω_n	ω_1	ω_2	η
1	44.00	43.65	44.36	0.0161
2	44.00	43.74	44.52	0.0177
3	44.00	43.67	44.33	0.0150
4	44.00	43.72	44.39	0.0152

Table 10: Sample A04 (25 mm, No Treatment, 27:100, 817 kg/m3)

Test #	ω_n	ω_1	ω_2	η
1	51.50	51.16	52.02	0.0167
2	51.50	51.24	52.15	0.0177
3	51.50	51.19	51.95	0.0148
4	51.50	51.26	52.07	0.0157

Table 11: Sample A05 (25 mm, No Treatment, 27:100, 1058 kg/m3)

Test #	ω_n	ω_1	ω_2	η
1	42.00	41.75	42.58	0.0198
2	42.00	41.79	42.66	0.0207
3	42.50	41.92	42.72	0.0188
4	42.50	41.93	42.72	0.0186

Table 12: Sample A06 (25 mm, No Treatment, 27:100, 1059 kg/m3)

Test #	ω_n	ω_1	ω_2	η
1	49.00	48.48	49.45	0.0198
2	49.00	48.74	49.73	0.0202
3	48.50	47.94	48.71	0.0159
4	48.50	47.99	48.76	0.0159

Table 13: Sample A07 (12.5 mm, No Treatment, 27:100, 1041 kg/m3)

Test #	ω_n	ω_1	ω_2	η
1	42.00	41.66	42.53	0.0207
2	42.00	41.73	42.61	0.0210
3	42.50	41.96	42.75	0.0186
4	42.50	41.97	42.77	0.0188

Table 14: Sample A08 (12.5 mm, No Treatment, 27:100, 1047 kg/m3)

Test #	ω_n	ω_1	ω_2	η
1	42.00	41.47	42.53	0.0252
2	42.00	41.53	42.58	0.0250
3	42.50	42.27	43.08	0.0191
4	42.50	42.29	43.14	0.0200

Table 15: Sample A09 (50 mm, No Treatment, 27:100, 1071 kg/m3)

Test #	ω_n	ω_1	ω_2	η
1	39.50	38.88	39.82	0.0238
2	39.50	39.10	40.04	0.0238
3	40.00	39.67	40.37	0.0175
4	40.00	39.73	40.50	0.0193

Table 16: Sample A10 (50 mm, No Treatment, 27:100, 1070 kg/m3)

Test #	ω_n	ω_1	ω_2	η
1	38.50	38.17	39.09	0.0239
2	39.00	38.24	39.23	0.0254
3	39.50	38.97	39.72	0.0190
4	39.50	39.06	39.76	0.0177

Table 17: Sample A11 (25 mm, No Treatment, 27:100, 1054 kg/m3)

Test #	ω_n	ω_1	ω_2	η
1	41.00	40.41	41.90	0.0363
2	41.50	40.96	42.40	0.0347
3	44.00	43.52	44.28	0.0173
4	43.00	42.42	43.22	0.0186

Table 18: Sample A12 (25 mm, No Treatment, 27:100, 1032 kg/m3)

Test #	ω_n	ω_1	ω_2	η
1	39.50	38.84	40.66	0.0461
2	43.50	43.19	43.99	0.0184
3	43.50	43.25	44.03	0.0179

Table 19: Sample A13 (25 mm, No Treatment, 29:100, 1053 kg/m3)

Test #	ω_n	ω_1	ω_2	η
1	33.00	32.27	33.20	0.0282
2	33.00	32.33	33.22	0.0270
3	33.00	32.64	33.31	0.0203
4	33.00	32.64	33.30	0.0200

Table 20: Sample A14 (25 mm, No Treatment, 29:100, 1064 kg/m3)

Test #	ω_n	ω_1	ω_2	η
1	38.50	37.94	38.86	0.0239
2	38.50	38.21	39.18	0.0252
3	38.50	37.99	38.78	0.0205
4	38.50	38.14	38.90	0.0197

Table 21: Sample A15 (25 mm, No Treatment, 25:100, 684 kg/m3)

Test #	ω_n	ω_1	ω_2	η
1	30.00	27.00	31.75	0.1583
2	29.00	26.25	31.20	0.1707
3	40.50	39.38	41.90	0.0622
4	41.50	39.88	42.63	0.0663

Table 22: Sample A16 (25 mm, No Treatment, 25:100, 673 kg/m3)

Test #	ω_n	ω_1	ω_2	η
1	29.00	25.40	31.25	0.2017
2	28.50	25.75	30.85	0.1789
3	41.00	39.48	42.69	0.0783
4	41.50	39.73	42.71	0.0718

Table 23: Sample A17 (25 mm, 5% NaOH, 27:100, 1106 kg/m3)

Test #	ω_n	ω_1	ω_2	η
1	29.00	28.68	29.59	0.0314
2	29.00	28.74	29.68	0.0324
3	30.00	29.41	30.18	0.0257
4	30.00	29.41	30.17	0.0253

Table 24: Sample A18 (25 mm, No Treatment, 27:100, 1072 kg/m3)

Test #	ω_n	ω_1	ω_2	η
1	33.50	32.99	34.01	0.0304
2	33.50	33.13	34.08	0.0284
3	35.50	34.93	35.80	0.0245
4	35.50	34.99	35.84	0.0239

Table 25: Sample A19 (25 mm, 5% NaOH , 27:100, 1112 kg/m3)

Test #	ω_n	ω_1	ω_2	η
1	33.50	32.85	34.14	0.0385
2	34.00	33.02	34.41	0.0409
3	37.00	35.97	37.65	0.0454
4	37.50	36.15	37.84	0.0451

Table 26: Sample A20 (25 mm, No Treatment, 27:100, 1025 kg/m3)

Test #	ω_n	ω_1	ω_2	η
1	36.00	35.15	36.61	0.0406
2	35.50	35.11	36.68	0.0442
3	39.00	38.44	39.58	0.0292
4	39.00	38.66	39.79	0.0290

Table 27: Sample A21 (25 mm, No Treatment, 26:100, 1013 kg/m3)

Test #	ω_n	ω_1	ω_2	η
1	38.5	38.04	39	0.0249
2	39	38.29	39.22	0.0238
3	39	38.64	39.42	0.0200
4	39	38.73	39.54	0.0208

Table 28: Sample A22 (25 mm, No Treatment, 26:100, 1039 kg/m3)

Test #	ω_n	ω_1	ω_2	η
1	35.5	35.16	36.17	0.0285
2	36	35.33	36.3	0.0269
3	35.5	34.83	35.78	0.0268
4	35.5	34.89	35.8	0.0256

Table 29: Sample A23 (25 mm, No Treatment, 24.5:100, 1069 kg/m3)

Test #	ω_n	ω_1	ω_2	η
1	38.5	37.64	39.02	0.0358
2	38.5	37.79	39.07	0.0332
3	40	39.64	40.55	0.0227
4	40	39.71	40.6	0.0223

Table 30: Sample A24 (25 mm, 3% NaOH, 27:100, 1097 kg/m3)

Test #	ω_n	ω_1	ω_2	η
1	33.00	32.41	33.36	0.0288
2	33.00	32.50	33.59	0.0330
3	35.00	34.68	35.73	0.0300
4	35.00	34.68	35.79	0.0317
5	35.50	35.19	36.21	0.0287
6	36.00	35.25	36.27	0.0283
7	36.00	35.32	36.28	0.0267
8	36.00	35.31	36.28	0.0269
9	36.50	36.10	37.11	0.0276
10	36.50	36.11	37.11	0.0274

Table 31: Sample A25 (25 mm, 8% NaOH, 27:100, 1058 kg/m^3)

Test #	ω_n	ω_1	ω_2	η
1	35.00	34.48	35.56	0.0309
2	35.00	34.49	35.73	0.0354
3	36.50	35.68	37.19	0.0414
4	36.50	35.80	37.62	0.0499
5	37.50	36.98	38.15	0.0312
6	37.50	37.16	38.19	0.0275
7	38.00	37.37	38.28	0.0239
8	38.00	37.45	38.42	0.0255
9	37.50	37.23	38.15	0.0245
10	37.50	37.31	38.22	0.0243

Appendix B

Mechanical Properties Grouped by Density

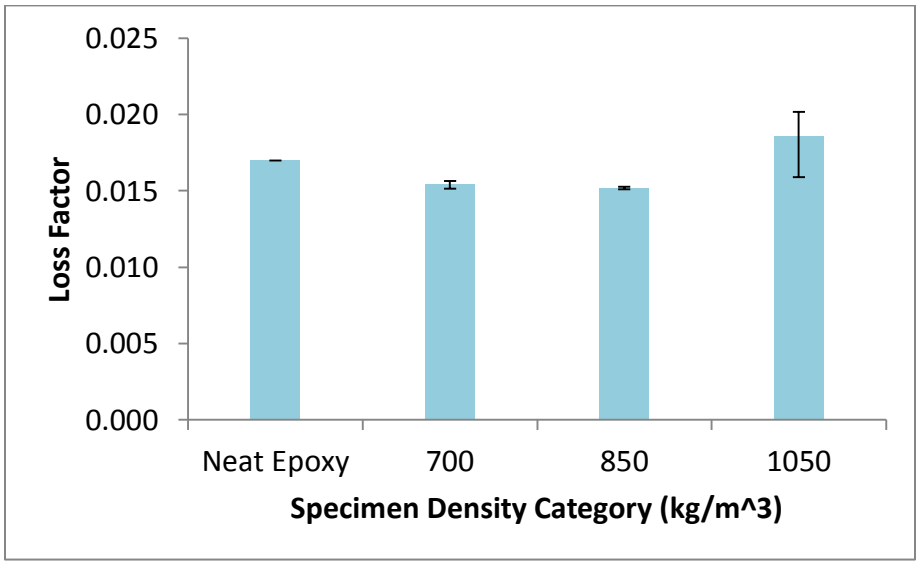

Figure 26: Loss Factor of Neat Epoxy and Composites Grouped by Density

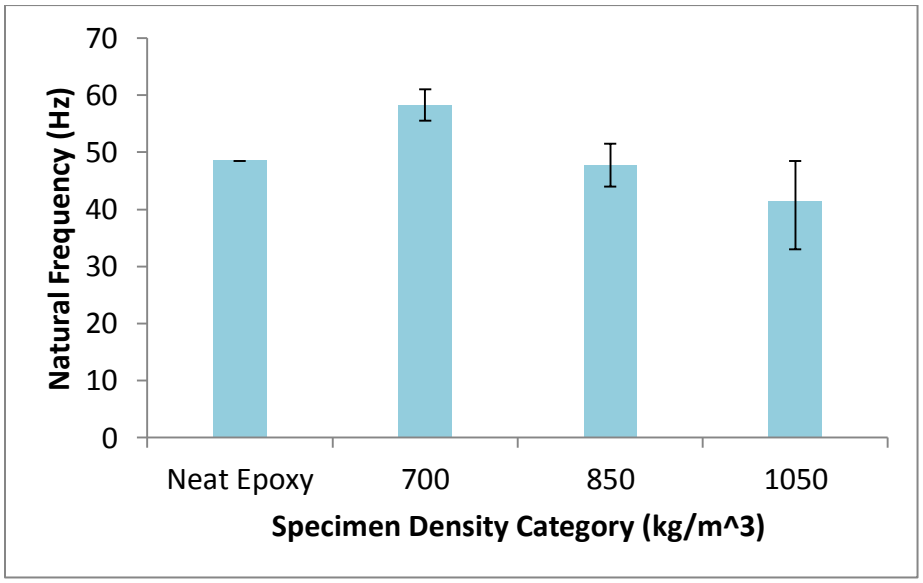

Figure 27: Natural Frequency of Neat Epoxy and Composites Grouped by Density

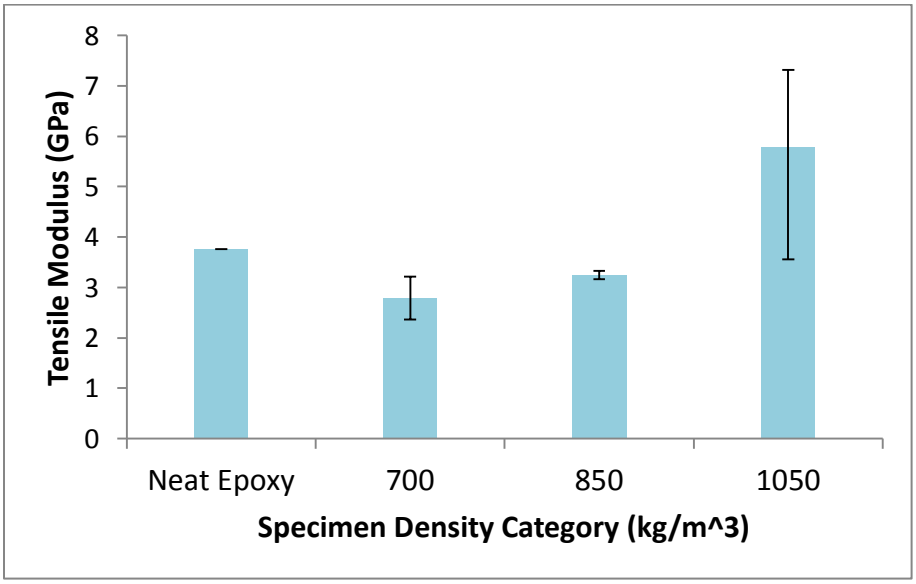

Figure 28: Tensile Modulus of Neat Epoxy and Composites Grouped by Density

Appendix C

Sensitivity Analysis Statistics

Table 32: The t-Ratios Associated with each Model Parameter

Model Parameter	t-Ratio
Fiber Radius	0.00
Matrix Shear Storage Modulus	-0.02
Interphase Volume Fraction	0.03
Matrix Radius	0.03
Fiber Length	-0.04
Matrix Volume Fraction	0.05
Interphase Storage Modulus	-0.14
Interphase Loss Modulus	0.14
Fiber Volume Fraction	0.33
Fiber Storage Modulus	-1.27
Fiber Loss Modulus	1.51
Matrix Loss Modulus	2.94
Matrix Storage Modulus	-3.18

Appendix D

FORTRAN Code: Calculating Loss Factor

```
Program Natural_Fiber_Damping_Sensitivity
Implicit None

Real :: l, rf, rm
Real :: vm, vf, vi
Real :: gpi, gppi, epf, eppf, epm, eppm, gpm
Real :: lo, rfo, rmo
Real :: vmo, vfo, vio
Real :: gpio, gppio, epfo, eppfo, epmo, eppmo, gpmo
Real :: beta, eti, etf
Real :: chyp, thyp
Real :: bl2, epc, eppc, etc


!ORIGINAL VALUES

lo=0.025            !Fiber Length
vfo=0.3             !Fiber Volume Fraction
vio=0.1             !Interphase Volume Fraction
vmo=1.-vfo-vio      !Matrix Volume Fraction
rfo=0.000045        !Fiber Radius
rmo=0.000082        !Matrix Radius
epmo=3.E9           !Matrix Storage Tensile Modulus
eppmo=0.15E9        !Matrix Loss Tensile Modulus
epfo=3.E9           !Fiber Storage Tensile Modulus
eppfo=0.18E9        !Fiber Loss Tensile Modulus
gpio=1.E6           !Interphase Storage Shear Modulus
gppio=0.1E6         !Interphase Loss Shear Modulus
gpmo=1.3E6          !Matrix Storage Shear Modulus

l=lo
vf=vfo
vi=vio
vm=vmo
rf=rfo
rm=rmo
epm=epmo
eppm=eppmo
epf=epfo
eppf=eppfo
```

```
gpi=gpio
gppi=gppio
gpm=gpmo

beta=SQRT( (2.*gpm) / (epf*rf*rf*log(rm/rf)) )
bl2=beta*l/2.
eti=gppi/gpi
etf=eppf/epf
chyp=cosh(bl2)
thyp=tanh(bl2)
epc=epf*vf*(1.-thyp/(bl2))-(eppf*vf/2.)*(eti-etf)*(thyp/(bl2)-1./(chyp**2))+epm*vm
eppc=eppf*vf*(1.-thyp/(bl2))+(epf*vf/2.)*(eti-etf)*(thyp/(bl2)-1./(chyp**2))+eppm*vm

etc=eppc/epc

Write(*,*) 'original = '
Write(*,*) ' '
Write(*,*) 'etc = '
Write(*,*) etc
Write(*,*) ' '


!ALTER l BY 10%

l=lo*1.1

beta=SQRT( (2.*gpm) / (epf*rf*rf*log(rm/rf)) )
bl2=beta*l/2.
eti=gppi/gpi
etf=eppf/epf
chyp=cosh(bl2)
thyp=tanh(bl2)
epc=epf*vf*(1.-thyp/(bl2))-(eppf*vf/2.)*(eti-etf)*(thyp/(bl2)-1./(chyp**2))+epm*vm
eppc=eppf*vf*(1.-thyp/(bl2))+(epf*vf/2.)*(eti-etf)*(thyp/(bl2)-1./(chyp**2))+eppm*vm

etc=eppc/epc

Write(*,*) 'l = '
Write(*,*) l
Write(*,*) ' '
Write(*,*) 'etc = '
Write(*,*) etc
Write(*,*) ' '

l=lo*0.9
```

```
beta=SQRT( (2.*gpm) / (epf*rf*rf*log(rm/rf)) )
bl2=beta*l/2.
eti=gppi/gpi
etf=eppf/epf
chyp=cosh(bl2)
thyp=tanh(bl2)
epc=epf*vf*(1.-thyp/(bl2))-(eppf*vf/2.)*(eti-etf)*(thyp/(bl2)-1./(chyp**2))+epm*vm
eppc=eppf*vf*(1.-thyp/(bl2))+(epf*vf/2.)*(eti-etf)*(thyp/(bl2)-1./(chyp**2))+eppm*vm

etc=eppc/epc

Write(*,*) 'l = '
Write(*,*) l
Write(*,*) ' '
Write(*,*) 'etc = '
Write(*,*) etc
Write(*,*) ' '


!ALTER vf BY 10%

l=lo
vf=vfo*1.1
vi=vio
vm=1.-vf-vi

beta=SQRT( (2.*gpm) / (epf*rf*rf*log(rm/rf)) )
bl2=beta*l/2.
eti=gppi/gpi
etf=eppf/epf
chyp=cosh(bl2)
thyp=tanh(bl2)
epc=epf*vf*(1.-thyp/(bl2))-(eppf*vf/2.)*(eti-etf)*(thyp/(bl2)-1./(chyp**2))+epm*vm
eppc=eppf*vf*(1.-thyp/(bl2))+(epf*vf/2.)*(eti-etf)*(thyp/(bl2)-1./(chyp**2))+eppm*vm

etc=eppc/epc

Write(*,*) 'vf = '
Write(*,*) vf
Write(*,*) ' '
Write(*,*) 'etc = '
Write(*,*) etc
Write(*,*) ' '
```

```
l=lo
vf=vfo*0.9
vi=vio
vm=1.-vf-vi

beta=SQRT( (2.*gpm) / (epf*rf*rf*log(rm/rf)) )
bl2=beta*l/2.
eti=gppi/gpi
etf=eppf/epf
chyp=cosh(bl2)
thyp=tanh(bl2)
epc=epf*vf*(1.-thyp/(bl2))-(eppf*vf/2.)*(eti-etf)*(thyp/(bl2)-1./(chyp**2))+epm*vm
eppc=eppf*vf*(1.-thyp/(bl2))+(epf*vf/2.)*(eti-etf)*(thyp/(bl2)-1./(chyp**2))+eppm*vm

etc=eppc/epc

Write(*,*) 'vf = '
Write(*,*) vf
Write(*,*) ' '
Write(*,*) 'etc = '
Write(*,*) etc
Write(*,*) ' '


!ALTER vi BY 10%

vf=vfo
vi=vio*1.1
vm=1.-vf-vi

beta=SQRT( (2.*gpm) / (epf*rf*rf*log(rm/rf)) )
bl2=beta*l/2.
eti=gppi/gpi
etf=eppf/epf
chyp=cosh(bl2)
thyp=tanh(bl2)
epc=epf*vf*(1.-thyp/(bl2))-(eppf*vf/2.)*(eti-etf)*(thyp/(bl2)-1./(chyp**2))+epm*vm
eppc=eppf*vf*(1.-thyp/(bl2))+(epf*vf/2.)*(eti-etf)*(thyp/(bl2)-1./(chyp**2))+eppm*vm

etc=eppc/epc

Write(*,*) 'vi = '
Write(*,*) vi
Write(*,*) ' '
Write(*,*) 'etc = '
```

```
Write(*,*) etc
Write(*,*) ' '

vf=vfo
vi=vio*0.9
vm=1.-vf-vi

beta=SQRT( (2.*gpm) / (epf*rf*rf*log(rm/rf)) )
bl2=beta*l/2.
eti=gppi/gpi
etf=eppf/epf
chyp=cosh(bl2)
thyp=tanh(bl2)
epc=epf*vf*(1.-thyp/(bl2))-(eppf*vf/2.)*(eti-etf)*(thyp/(bl2)-1./(chyp**2))+epm*vm
eppc=eppf*vf*(1.-thyp/(bl2))+(epf*vf/2.)*(eti-etf)*(thyp/(bl2)-1./(chyp**2))+eppm*vm

etc=eppc/epc

Write(*,*) 'vi = '
Write(*,*) vi
Write(*,*) ' '
Write(*,*) 'etc = '
Write(*,*) etc
Write(*,*) ' '


!ALTER vm BY 10%

vm=vmo*1.1
vf=vfo-vmo*.55
vi=vio-vmo*.55

beta=SQRT( (2.*gpm) / (epf*rf*rf*log(rm/rf)) )
bl2=beta*l/2.
eti=gppi/gpi
etf=eppf/epf
chyp=cosh(bl2)
thyp=tanh(bl2)
epc=epf*vf*(1.-thyp/(bl2))-(eppf*vf/2.)*(eti-etf)*(thyp/(bl2)-1./(chyp**2))+epm*vm
eppc=eppf*vf*(1.-thyp/(bl2))+(epf*vf/2.)*(eti-etf)*(thyp/(bl2)-1./(chyp**2))+eppm*vm

etc=eppc/epc

Write(*,*) 'vm = '
Write(*,*) vm
```

```
Write(*,*) ' '
Write(*,*) 'etc = '
Write(*,*) etc
Write(*,*) ' '

vm=vmo*0.9
vf=vfo-vmo*.55
vi=vio-vmo*.55

beta=SQRT( (2.*gpm) / (epf*rf*rf*log(rm/rf)) )
bl2=beta*l/2.
eti=gppi/gpi
etf=eppf/epf
chyp=cosh(bl2)
thyp=tanh(bl2)
epc=epf*vf*(1.-thyp/(bl2))-(eppf*vf/2.)*(eti-etf)*(thyp/(bl2)-1./(chyp**2))+epm*vm
eppc=eppf*vf*(1.-thyp/(bl2))+(epf*vf/2.)*(eti-etf)*(thyp/(bl2)-1./(chyp**2))+eppm*vm

etc=eppc/epc

Write(*,*) 'vm = '
Write(*,*) vm
Write(*,*) ' '
Write(*,*) 'etc = '
Write(*,*) etc
Write(*,*) ' '


!ALTER epm BY 10%

vf=vfo
vi=vio
vm=vmo
epm=epmo*1.1

beta=SQRT( (2.*gpm) / (epf*rf*rf*log(rm/rf)) )
bl2=beta*l/2.
eti=gppi/gpi
etf=eppf/epf
chyp=cosh(bl2)
thyp=tanh(bl2)
epc=epf*vf*(1.-thyp/(bl2))-(eppf*vf/2.)*(eti-etf)*(thyp/(bl2)-1./(chyp**2))+epm*vm
eppc=eppf*vf*(1.-thyp/(bl2))+(epf*vf/2.)*(eti-etf)*(thyp/(bl2)-1./(chyp**2))+eppm*vm

etc=eppc/epc
```

```
Write(*,*) 'epm = '
Write(*,*) epm
Write(*,*) ' '
Write(*,*) 'etc = '
Write(*,*) etc
Write(*,*) ' '

vf=vfo
vi=vio
vm=vmo
epm=epmo*0.9

beta=SQRT( (2.*gpm) / (epf*rf*rf*log(rm/rf)) )
bl2=beta*l/2.
eti=gppi/gpi
etf=eppf/epf
chyp=cosh(bl2)
thyp=tanh(bl2)
epc=epf*vf*(1.-thyp/(bl2))-(eppf*vf/2.)*(eti-etf)*(thyp/(bl2)-1./(chyp**2))+epm*vm
eppc=eppf*vf*(1.-thyp/(bl2))+(epf*vf/2.)*(eti-etf)*(thyp/(bl2)-1./(chyp**2))+eppm*vm

etc=eppc/epc

Write(*,*) 'epm = '
Write(*,*) epm
Write(*,*) ' '
Write(*,*) 'etc = '
Write(*,*) etc
Write(*,*) ' '


!ALTER eppm BY 10%

epm=epmo
eppm=eppmo*1.1

beta=SQRT( (2.*gpm) / (epf*rf*rf*log(rm/rf)) )
bl2=beta*l/2.
eti=gppi/gpi
etf=eppf/epf
chyp=cosh(bl2)
thyp=tanh(bl2)
epc=epf*vf*(1.-thyp/(bl2))-(eppf*vf/2.)*(eti-etf)*(thyp/(bl2)-1./(chyp**2))+epm*vm
eppc=eppf*vf*(1.-thyp/(bl2))+(epf*vf/2.)*(eti-etf)*(thyp/(bl2)-1./(chyp**2))+eppm*vm
```

```
etc=eppc/epc

Write(*,*) 'eppm = '
Write(*,*) eppm
Write(*,*) ' '
Write(*,*) 'etc = '
Write(*,*) etc
Write(*,*) ' '

epm=epmo
eppm=eppmo*0.9

beta=SQRT( (2.*gpm) / (epf*rf*rf*log(rm/rf)) )
bl2=beta*l/2.
eti=gppi/gpi
etf=eppf/epf
chyp=cosh(bl2)
thyp=tanh(bl2)
epc=epf*vf*(1.-thyp/(bl2))-(eppf*vf/2.)*(eti-etf)*(thyp/(bl2)-1./(chyp**2))+epm*vm
eppc=eppf*vf*(1.-thyp/(bl2))+(epf*vf/2.)*(eti-etf)*(thyp/(bl2)-1./(chyp**2))+eppm*vm

etc=eppc/epc

Write(*,*) 'eppm = '
Write(*,*) eppm
Write(*,*) ' '
Write(*,*) 'etc = '
Write(*,*) etc
Write(*,*) ' '


!ALTER epf BY 10%

eppm=eppmo
epf=epfo*1.1

beta=SQRT( (2.*gpm) / (epf*rf*rf*log(rm/rf)) )
bl2=beta*l/2.
eti=gppi/gpi
etf=eppf/epf
chyp=cosh(bl2)
thyp=tanh(bl2)
epc=epf*vf*(1.-thyp/(bl2))-(eppf*vf/2.)*(eti-etf)*(thyp/(bl2)-1./(chyp**2))+epm*vm
eppc=eppf*vf*(1.-thyp/(bl2))+(epf*vf/2.)*(eti-etf)*(thyp/(bl2)-1./(chyp**2))+eppm*vm
```

```
etc=eppc/epc

Write(*,*) 'epf = '
Write(*,*) epf
Write(*,*) ' '
Write(*,*) 'etc = '
Write(*,*) etc
Write(*,*) ' '

eppm=eppmo
epf=epfo*0.9

beta=SQRT( (2.*gpm) / (epf*rf*rf*log(rm/rf)) )
bl2=beta*l/2.
eti=gppi/gpi
etf=eppf/epf
chyp=cosh(bl2)
thyp=tanh(bl2)
epc=epf*vf*(1.-thyp/(bl2))-(eppf*vf/2.)*(eti-etf)*(thyp/(bl2)-1./(chyp**2))+epm*vm
eppc=eppf*vf*(1.-thyp/(bl2))+(epf*vf/2.)*(eti-etf)*(thyp/(bl2)-1./(chyp**2))+eppm*vm

etc=eppc/epc

Write(*,*) 'epf = '
Write(*,*) epf
Write(*,*) ' '
Write(*,*) 'etc = '
Write(*,*) etc
Write(*,*) ' '


!ALTER eppf BY 10%

epf=epfo
eppf=eppfo*1.1

beta=SQRT( (2.*gpm) / (epf*rf*rf*log(rm/rf)) )
bl2=beta*l/2.
eti=gppi/gpi
etf=eppf/epf
chyp=cosh(bl2)
thyp=tanh(bl2)
epc=epf*vf*(1.-thyp/(bl2))-(eppf*vf/2.)*(eti-etf)*(thyp/(bl2)-1./(chyp**2))+epm*vm
eppc=eppf*vf*(1.-thyp/(bl2))+(epf*vf/2.)*(eti-etf)*(thyp/(bl2)-1./(chyp**2))+eppm*vm
```

```
etc=eppc/epc

Write(*,*) 'eppf = '
Write(*,*) eppf
Write(*,*) ' '
Write(*,*) 'etc = '
Write(*,*) etc
Write(*,*) ' '

epf=epfo
eppf=eppfo*0.9

beta=SQRT( (2.*gpm) / (epf*rf*rf*log(rm/rf)) )
bl2=beta*l/2.
eti=gppi/gpi
etf=eppf/epf
chyp=cosh(bl2)
thyp=tanh(bl2)
epc=epf*vf*(1.-thyp/(bl2))-(eppf*vf/2.)*(eti-etf)*(thyp/(bl2)-1./(chyp**2))+epm*vm
eppc=eppf*vf*(1.-thyp/(bl2))+(epf*vf/2.)*(eti-etf)*(thyp/(bl2)-1./(chyp**2))+eppm*vm

etc=eppc/epc

Write(*,*) 'eppf = '
Write(*,*) eppf
Write(*,*) ' '
Write(*,*) 'etc = '
Write(*,*) etc
Write(*,*) ' '


!ALTER gpi BY 10%

eppf=eppfo
gpi=gpio*1.1

beta=SQRT( (2.*gpm) / (epf*rf*rf*log(rm/rf)) )
bl2=beta*l/2.
eti=gppi/gpi
etf=eppf/epf
chyp=cosh(bl2)
thyp=tanh(bl2)
epc=epf*vf*(1.-thyp/(bl2))-(eppf*vf/2.)*(eti-etf)*(thyp/(bl2)-1./(chyp**2))+epm*vm
eppc=eppf*vf*(1.-thyp/(bl2))+(epf*vf/2.)*(eti-etf)*(thyp/(bl2)-1./(chyp**2))+eppm*vm
```

```
etc=eppc/epc

Write(*,*) 'gpi = '
Write(*,*) gpi
Write(*,*) ' '
Write(*,*) 'etc = '
Write(*,*) etc
Write(*,*) ' '

eppf=eppfo
gpi=gpio*0.9

beta=SQRT( (2.*gpm) / (epf*rf*rf*log(rm/rf)) )
bl2=beta*l/2.
eti=gppi/gpi
etf=eppf/epf
chyp=cosh(bl2)
thyp=tanh(bl2)
epc=epf*vf*(1.-thyp/(bl2))-(eppf*vf/2.)*(eti-etf)*(thyp/(bl2)-1./(chyp**2))+epm*vm
eppc=eppf*vf*(1.-thyp/(bl2))+(epf*vf/2.)*(eti-etf)*(thyp/(bl2)-1./(chyp**2))+eppm*vm

etc=eppc/epc

Write(*,*) 'gpi = '
Write(*,*) gpi
Write(*,*) ' '
Write(*,*) 'etc = '
Write(*,*) etc
Write(*,*) ' '


!ALTER gppi BY 10%

gpi=gpio
gppi=gppio*1.1

beta=SQRT( (2.*gpm) / (epf*rf*rf*log(rm/rf)) )
bl2=beta*l/2.
eti=gppi/gpi
etf=eppf/epf
chyp=cosh(bl2)
thyp=tanh(bl2)
epc=epf*vf*(1.-thyp/(bl2))-(eppf*vf/2.)*(eti-etf)*(thyp/(bl2)-1./(chyp**2))+epm*vm
eppc=eppf*vf*(1.-thyp/(bl2))+(epf*vf/2.)*(eti-etf)*(thyp/(bl2)-1./(chyp**2))+eppm*vm
```

```
etc=eppc/epc

Write(*,*) 'gppi = '
Write(*,*) gppi
Write(*,*) ' '
Write(*,*) 'etc = '
Write(*,*) etc
Write(*,*) ' '

gpi=gpio
gppi=gppio*0.9

beta=SQRT( (2.*gpm) / (epf*rf*rf*log(rm/rf)) )
bl2=beta*l/2.
eti=gppi/gpi
etf=eppf/epf
chyp=cosh(bl2)
thyp=tanh(bl2)
epc=epf*vf*(1.-thyp/(bl2))-(eppf*vf/2.)*(eti-etf)*(thyp/(bl2)-1./(chyp**2))+epm*vm
eppc=eppf*vf*(1.-thyp/(bl2))+(epf*vf/2.)*(eti-etf)*(thyp/(bl2)-1./(chyp**2))+eppm*vm

etc=eppc/epc

Write(*,*) 'gppi = '
Write(*,*) gppi
Write(*,*) ' '
Write(*,*) 'etc = '
Write(*,*) etc
Write(*,*) ' '


!ALTER gpm BY 10%

gppi=gppio
gpm=gpmo*1.1

beta=SQRT( (2.*gpm) / (epf*rf*rf*log(rm/rf)) )
bl2=beta*l/2.
eti=gppi/gpi
etf=eppf/epf
chyp=cosh(bl2)
thyp=tanh(bl2)
epc=epf*vf*(1.-thyp/(bl2))-(eppf*vf/2.)*(eti-etf)*(thyp/(bl2)-1./(chyp**2))+epm*vm
eppc=eppf*vf*(1.-thyp/(bl2))+(epf*vf/2.)*(eti-etf)*(thyp/(bl2)-1./(chyp**2))+eppm*vm
```

```
etc=eppc/epc

Write(*,*) 'gpm = '
Write(*,*) gpm
Write(*,*) ' '
Write(*,*) 'etc = '
Write(*,*) etc
Write(*,*) ' '

gppi=gppio
gpm=gpmo*0.9

beta=SQRT( (2.*gpm) / (epf*rf*rf*log(rm/rf)) )
bl2=beta*l/2.
eti=gppi/gpi
etf=eppf/epf
chyp=cosh(bl2)
thyp=tanh(bl2)
epc=epf*vf*(1.-thyp/(bl2))-(eppf*vf/2.)*(eti-etf)*(thyp/(bl2)-1./(chyp**2))+epm*vm
eppc=eppf*vf*(1.-thyp/(bl2))+(epf*vf/2.)*(eti-etf)*(thyp/(bl2)-1./(chyp**2))+eppm*vm

etc=eppc/epc

Write(*,*) 'gpm = '
Write(*,*) gpm
Write(*,*) ' '
Write(*,*) 'etc = '
Write(*,*) etc
Write(*,*) ' '


!ALTER rf BY 10%

gpm=gpmo
rf=rfo*1.1

beta=SQRT( (2.*gpm) / (epf*rf*rf*log(rm/rf)) )
bl2=beta*l/2.
eti=gppi/gpi
etf=eppf/epf
chyp=cosh(bl2)
thyp=tanh(bl2)
epc=epf*vf*(1.-thyp/(bl2))-(eppf*vf/2.)*(eti-etf)*(thyp/(bl2)-1./(chyp**2))+epm*vm
eppc=eppf*vf*(1.-thyp/(bl2))+(epf*vf/2.)*(eti-etf)*(thyp/(bl2)-1./(chyp**2))+eppm*vm
```

```
etc=eppc/epc

Write(*,*) 'rf = '
Write(*,*) rf
Write(*,*) ' '
Write(*,*) 'etc = '
Write(*,*) etc
Write(*,*) ' '

gpm=gpmo
rf=rfo*0.9

beta=SQRT( (2.*gpm) / (epf*rf*rf*log(rm/rf)) )
bl2=beta*l/2.
eti=gppi/gpi
etf=eppf/epf
chyp=cosh(bl2)
thyp=tanh(bl2)
epc=epf*vf*(1.-thyp/(bl2))-(eppf*vf/2.)*(eti-etf)*(thyp/(bl2)-1./(chyp**2))+epm*vm
eppc=eppf*vf*(1.-thyp/(bl2))+(epf*vf/2.)*(eti-etf)*(thyp/(bl2)-1./(chyp**2))+eppm*vm

etc=eppc/epc

Write(*,*) 'rf = '
Write(*,*) rf
Write(*,*) ' '
Write(*,*) 'etc = '
Write(*,*) etc
Write(*,*) ' '


!ALTER rm BY 10%

rf=rfo
rm=rmo*1.1

beta=SQRT( (2.*gpm) / (epf*rf*rf*log(rm/rf)) )
bl2=beta*l/2.
eti=gppi/gpi
etf=eppf/epf
chyp=cosh(bl2)
thyp=tanh(bl2)
epc=epf*vf*(1.-thyp/(bl2))-(eppf*vf/2.)*(eti-etf)*(thyp/(bl2)-1./(chyp**2))+epm*vm
eppc=eppf*vf*(1.-thyp/(bl2))+(epf*vf/2.)*(eti-etf)*(thyp/(bl2)-1./(chyp**2))+eppm*vm
```

```
etc=eppc/epc

Write(*,*) 'rm = '
Write(*,*) rm
Write(*,*) ' '
Write(*,*) 'etc = '
Write(*,*) etc
Write(*,*) ' '

rf=rfo
rm=rmo*0.9

beta=SQRT( (2.*gpm) / (epf*rf*rf*log(rm/rf)) )
bl2=beta*l/2.
eti=gppi/gpi
etf=eppf/epf
chyp=cosh(bl2)
thyp=tanh(bl2)
epc=epf*vf*(1.-thyp/(bl2))-(eppf*vf/2.)*(eti-etf)*(thyp/(bl2)-1./(chyp**2))+epm*vm
eppc=eppf*vf*(1.-thyp/(bl2))+(epf*vf/2.)*(eti-etf)*(thyp/(bl2)-1./(chyp**2))+eppm*vm

etc=eppc/epc

Write(*,*) 'rm = '
Write(*,*) rm
Write(*,*) ' '
Write(*,*) 'etc = '
Write(*,*) etc
Write(*,*) ' '


End Program
```